The GPR17 receptor in NG2 expressing cells: Focus on in vivocell maturation and participation in acute trauma and chronic damage

(Article begins on next page)

19 October 2024

The GPR17 receptor in NG2 expressing cells: focus on in vivo cell maturation and participation in acute trauma and chronic damage

The GPR17 receptor in NG2 expressing cells: focus on in vivo cell maturation and participation in acute trauma and chronic damage

Enrica Boda[1, 2]*, Francesca Viganò[3,4]*, Patrizia Rosa[5], Marta Fumagalli[3], Vivien Labat-gest[1, 2], Filippo Tempia[1, 2, 6], Maria P. Abbracchio[3], Leda Dimou[4] and Annalisa Buffo[1, 2, 7]

[1]Department of Neuroscience, University of Turin, Turin, Italy

[2]Neuroscience Institute Cavalieri-Ottolenghi (NICO), Regione Gonzole 10 10043 Orbassano Turin, Italy

[3]Laboratory of Molecular and Cellular Pharmacology of Purinergic Transmission, Department of Pharmacological Sciences, University of Milan, Italy

[4]Institute of Physiology, Physiological Genomics, Ludwig-Maximilians-University, Pettenkoferstr. 12, 80336 Munich, Germany

[5]CNR Institute of Neuroscience, Department of Medical Pharmacology, Via Vanvitelli 32, Milan, Italy

[6]National Institute of Neuroscience-Italy (INN), Turin, Italy

[7]Neuroscience Institute of Turin (NIT), Turin, Italy

* These authors contributed equally to the work

Running title: GPR17 in NG2 expressing cells

Number of words in abstract, 250; introduction, 542; materials and methods: 1642; results, 3561; discussion, 1464; figure legends, 1461; references, 1797.

Total word number, 10467.

Figures, 7

Tables, 1

Supporting Information, 7 figures and legends, 2 tables

Author for correspondence:

Annalisa Buffo

Department of Neuroscience, University of Turin, Neuroscience Institute Cavalieri-Ottolenghi,

Neuroscience Institute of Turin

Regione Gonzole 10 10043 Orbassano Turin – Italy

Tel 00 39 011 6706614

Fax 00 39 011 6705449

Email: annalisa.buffo@unito.it

Keywords: NG2+ cells; oligodendrocyte development; glial reactivity; demyelination; mouse neocortex

Abbreviations: +, positive; BrdU, 5-bromo-2-deoxyuridine; CNS, central nervous system; CTRL, contralateral; DAPI, 4',6-diamidino-2-phenylindole; d, days;dpi, days post injection; dpl, days post lesion; dpt, days post BrdU treatment; GM, gray matter; Grm, GPR17 receptor on cell membrane; GPR17, G-protein coupled receptor 17; Gpi, GPR17 protein intracellular; GST-π, glutathione S-transferase-π; h, hours; MAG, myelin associated glycoprotein; MBP, myelin basic protein; P, postnatal day; PLP1, proteolipid protein 1; RIP, 2',3'-cyclic nucleotide 3'-phosphodiesterase; RT, reverse-transcription; SW, stab-wound; wks, weeks; WM, white matter; WT, wild type.

Abstract

NG2-expressing cells comprise a population of cycling precursors that can exit the cell cycle and differentiate into mature oligodendrocytes. As a whole, they display heterogeneous properties and behaviours that remain unresolved at the molecular level, although partly interpretable as distinct maturation stages. To address this issue, we analyzed the expression of the GPR17 receptor, recently shown to decorate NG2-expressing cells and to operate as an early sensor of brain damage, in immature and adult oligodendrocyte progenitors in the intact brain and after injury. In both the early postnatal and adult cerebral cortex, distinct GPR17 protein localisations and expression levels define different stages of oligodendroglial maturation, ranging from the precursor phase to the premyelinating phenotype. As soon as cells exit mitosis, a fraction of NG2-expressing cells displays accumulation of GPR17 protein in the Golgi apparatus. GPR17 expression is subsequently upregulated and distributed to processes of cells that stop dividing, progressively lose NG2 positivity and assume pre-myelinating features. Absence of colabelling with mature markers or myelin proteins indicates that GPR17 is downregulated when cells complete their final maturation. BrdU-based fate-mapping demonstrated that a significant fraction of newly generated oligodendrocyte progenitors transiently upregulates GPR17 during their maturation. Importantly, we also found that GPR17 does not participate to the early reaction of NG2-expressing cells to damage, while it is induced at post-acute stages after injury. These findings identify GPR17 as a marker for progenitor progression within the oligodendroglial lineage and highlight its participation to post-acute reactivity of NG2 cells in different injury paradigms.

Introduction

Cells expressing the chrondroitin sulphate proteoglycan NG2 and displaying traits of the oligodendroglial lineage comprise an abundant population in the immature and adult central nervous system (CNS) (Butt et al., 2002; Nishiyama et al., 2002). These cells behave as precursors for mature oligodendrocytes *in vitro* and *in vivo*, and potentially for astrocytes and neurons (Nishiyama 2009; Boda and Buffo, 2010; Trotter et al., 2010). Furthermore, they represent the major population of cycling cells in the adult nervous tissue (Horner et al., 2000; Dawson et al., 2003; Simon et al., 2011), and respond to injury by increased proliferation (Butt et al., 2002; Simon et al., 2011). Notably, their multiple functions also encompass a tight interplay with neurons by synaptic signalling, expression of neurotransmitter receptors and generation of action potentials (Bakiri et al., 2009).

However, it is increasingly clear that NG2 positive (+) cells possess heterogeneous properties and behaviours, as indicated by myelination abilities in the adult gray and white matter (Dimou et al., 2008; Rivers et al., 2008), proliferative activity (reviewed in Nishiyama et al., 2009), response to neuronal activity (De Biase et al., 2010) and reaction to injury (Hampton et al., 2004; Lytle et al., 2009). Such diversity can be partly explained by distinct maturation stages (De Biase et al., 2010), but molecular markers are lacking to unambiguously resolve this point.

With the aim to gain insights into NG2+ cell heterogeneity, we focused on the G-protein coupled GPR17 receptor, which has been recently shown to be expressed by oligodendrocyte precursor cells (Lecca et al., 2008) and recognized as an interesting functional oligodendroglial modulator (Lecca et al., 2008; Chen et al., 2009; Fumagalli et al., 2011). GPR17 is activated by uracil nucleotides and cysteinyl leukotrienes (Ciana et al., 2006; Lecca et al., 2008; Pugliese et al., 2009). While uracil nucleotides and their sugar conjugates are gaining importance as

signalling mediators in the healthy CNS (Lecca and Ceruti, 2008), both classes of GPR17 endogenous agonists are massively released at the site of injury in traumatic, vascular and inflammatory pathologies (Ciceri et al., 2001; Melani et al., 2005; Buffo et al., 2010), where they activate tissue reactivity. GPR17 was shown to operate as a "sensor molecule" for these damage signals, orchestrating the early CNS reaction to stroke and spinal cord injury (Ciana et al., 2006; Lecca et al., 2008; Ceruti et al., 2009). These studies, however, did not examine whether GPR17 was specifically implicated in activating the response of NG2+ cells to injury. Further, it has remained so far undefined at which exact phase of oligodendroglial maturation the receptor is acting *in vivo*, and how GPR17 expressing cells behave during postnatal ontogenesis.

To address these issues, we i) analysed the expression pattern and the proliferative behaviour of GPR17+ oligodendroglial cells in the postnatal and adult mouse cerebral cortex in the intact brain; ii) extended this analysis to models of traumatic brain injury and cerebral amiloidosis so to gain insights into the participation of GPR17 in the reaction of NG2+ cells to acute and chronic damage. We found that GPR17 transiently labels relevant fractions of NG2+ cells that upregulate the receptor after cell division and progress to the premyelinating stage. Furthermore, we show that GPR17 induction participates in the post-acute response to damage of oligodendroglial cells.

MATERIALS AND METHODS

Animals and surgical procedures

All experiments were performed on C57BL/6 mice (early postnatal and adult). Surgical procedures and perfusions were carried out under deep general anaesthesia (ketamine, 100 mg/kg; Ketavet, Bayern, Leverkusen, Germany; xylazine, 5 mg/kg; Rompun; Bayer, Milan, Italy). The experimental plan was designed according to the guidelines of the NIH, the European Communities Council (86/609/EEC), the state of Bavaria (under licence number 55.2-1-54-2531-144/07), the Italian law for care and use of experimental animals (DL116/92). It was also approved by the Italian Ministry of Health and the Bioethical Committee of the University of Turin.

Two-to-four month old mice underwent a stab-wound in the right cerebral cortex (Bregma from -0.4 mm to -2 mm, latero-lateral 1.5–2.5 mm) encompassing both gray and white matter and were sacrificed at different time-points after lesion (see results). As a model of chronic amyloid deposition, we examined 12 month-old C57BL/6-TgN (Thy1-APP$_{KM670/671NL}$; Thy1-PS1$_{L166P}$) mice (APPPS1) and wild-type littermates (Radde et al, 2006).

Proliferation, fate analysis and immunohistochemistry

To examine cell proliferation in intact, stab-wounded and APPPS1 mice we employed the thymidine analogue 5-bromo-2-deoxyuridine (BrdU, Sigma Aldrich, Milan, Italy), that is incorporated in the DNA during the S-phase of the cell cycle and remains into the DNA even when the cell exits the active phase of the cells cycle, therefore being suitable to detect not only active mitosis but also cells that had proliferated at the moment of BrdU administration (see Supp. Info. Fig. 1A; Buffo et al., 2005; Taupin, 2007; Dimou et al., 2008). Active proliferation (fast-proliferating cells) at the moment of analysis was revealed by either two

subsequent BrdU injections (100 mg/kg body weight for adult mice or 50 mg/kg body weight for pups, i.p.) performed at a 2 hour distance followed by sacrifice 2 hours after the last pulse, or by expression of Ki67 (an antigen present from S to M phases of the cell cycle, Taupin, 2007). To tag all cells that had proliferated within a defined time-window (including fast- and slow-proliferating cells as well as their post-mitotic progeny), BrdU (1mg/ml) was administered in drinking water until sacrifice. In case of stab-wound injury, BrdU treatment was initiated immediately after lesion. The kinetics of GPR17 expression in newly generated cells were evaluated by BrdU retaining after a double BrdU pulse (see above, 3 day old pups and adult mice) or after BrdU administration for 2 weeks (adult mice). BrdU incorporation into GPR17+ cells was assessed immediately after treatment and at different survival times (Supp. Info. Fig. 1A).

For histological analysis, animals were anaesthetized (as above) and transcardially perfused with 4% paraformaldehyde in phosphate buffer. Brains were postfixed, cryoprotected, and processed according to standard protocols (Buffo et al., 2005; Dimou et al., 2008). Adult brains were cut in 30 μm thick coronal sections collected in PBS. Brain slices of mice up to 14 days after birth (P14) were placed directly onto glass slides. The sections were stained to detect the expression of different antigens (see Supp. Info. Table1). Incubation with primary antibodies was made overnight at 4°C in PBS with 1.5% goat normal serum and 0.5% Triton-X 100. The sections were then exposed for two hours at room temperature to secondary antibodies (Supp. Info. Table 2). 4',6-diamidino-2-phenylindole (DAPI, Fluka, Milan, Italy) was used to visualize cell nuclei. Some sections were stained with the ApopTag fluorescein in situ apoptosis detection kit (Chemicon) to detect apoptotic cells. After processing, sections were mounted on microscope slides with Tris-glycerol supplemented with 10% Mowiol (Calbiochem, LaJolla, CA) or Aquapolymount (Hiss).

GPR17 was detected by means of affinity-purified antibodies (Supp. Info. Table 1; Ciana et al., 2006). Specificity of the "in house-made" antibody was tested by western blot analysis of total homogenates from Oli-neu cells, a mouse oligodendroglial cell line (Jung et al., 1995), transfected with a siRNA against the GPR17 gene (E. Parmigiani et al., unpublished). To reveal GPR17 expression either standard immunofluorescence procedures were applied (see above) or, for costaining of primary antibodies developed in the same species, the high sensitivity tyramide signal amplification kit (Perkin Elmer, Monza, Italy) was utilized according to the manufacturer's instruction (see also Buffo et al., 2005). NG2 expression was evaluated and confirmed with both rabbit and rat (AN2 clone) antibodies (Supp. Info. Table 1) that yielded comparable results. Stainings for CD9 and PLP/DM20 were performed as in Kukley et al. (2010). For PDGFRa labelling, post-fixation after perfusion was omitted. To facilitate BrdU recognition, slices were either treated with 2N HCl for 20 minutes at 37°C, followed by 10 minutes in borate buffer, or boiled for 20 minutes in citrate buffer before adding primary antibodies. This latter procedure was also applied for anti-Ki67 staining.

Primary oligodendrocyte precursor cultures

Primary cultures of oligodendrocyte precursors belonged to a previous set of experiments (Fumagalli et al., 2011). Coverslips stained with the anti-GPR17 antibody and mouse anti-NG2 antibody (1:200, Abcam, Cambridge, UK) were re-evaluated to assess the presence of the GPR17 protein in oligodendrocyte precursor somata.

Real time RT-PCR

Quantitative Real Time RT-PCR experiments were performed as in Boda et al., 2009. Briefly, mice (4-6 individuals per time point and experimental condition) were sacrificed (see above),

brains quickly removed under semi-sterile conditions and placed in ice-cold standard Ringer solution bubbled with 95% O_2- 5% CO_2. Thereafter, 400 μm thick coronal sections were prepared using a vibratome (Leica Microsystems GmbH, Wetzlar, Germany) and small pieces of intact or stab-wounded neocortex including the underlying white matter (WM) were dissected out and immediately frozen in -80°C 2-methylbutane before total RNA isolation (RNeasy micro kit, Qiagen, Milan, Italy). One μg of total RNA was reverse-transcribed (RT) to single stranded cDNA (High-Capacity cDNA Archive Kit, Applied Biosystems, Monza, Italy).

An ABI Prism 7000 Sequence Detection System (Applied Biosystems) was employed in combination with Taqman reagent-based chemistry (Applied Biosystems). Commercial Taqman Gene Expression Assays were purchased from Applied Biosystems to determine the amount of GPR17 (Mm02619401_s1) and the housekeeping genes glyceraldehyde-3-phosphate dehydrogenase (Gapdh, Mm99999915_g1) and beta-actin (Actb, Mm00607939_s1). PCR amplifications were run in duplicate. Blank controls consisting in no template (water) or RT-negative reactions were performed for each run. Data extracted from each real time RT-PCR run were analysed by means of the 7000 v1.1 SDS instrument software (Applied Biosystems). A relative quantification approach was used, according to the 2^{-ddCT} method (Livak and Schmittgen, 2001). Suitable housekeeping genes were selected following Boda et al. (2009). On this basis, Gapdh was used for the quantifications of samples from cortical stab-wounds and controls, Actb for samples from APPPS1 and wild type mice.

Western Blot analysis

Brains from postnatal mice were extracted and rapidly frozen at -80°C. Membrane protein extracts were obtained by tissue homogenization in buffer A (50 mM Tris HCl, pH 7.4, 150 mM NaCl, 2mM EGTA and protease inhibitor cocktail, Sigma). The homogenate was centrifuged at

800 g for 10 min at 4°C, and the postnuclear supernatant was centrifuged at 200.000 g for 1 h at 4°C to generate membrane and cytosolic fractions. The membrane fractions were solubilised in buffer A containing 1% TritonX-100. The protein concentration was estimated using the Bio-Rad Protein Assay (Bio-Rad Laboratories s.r.l., Segrate, Italy). Western blot was performed as previously described (Taverna et al., 2004). Briefly, equal amounts of proteins (30 μg) for each sample were loaded on 10% SDS-PAGE and then blotted onto nitrocellulose filters (Invitrogen, San Giuliano Milanese, Italy). After blocking with 5% dry milk in TBS buffer (20 mM Tris pH 7.4, 150 mM NaCl), filters were probed with anti-GPR17 (1:1000), anti-Actin (mouse monoclonal 1:3000, Sigma) and anti-myelin associated glycoprotein (MAG) (mouse monoclonal 1:1000; Chemicon, Temecula, CA) antibodies diluted in TBS buffer containing 5% milk and 0.3% Tween 20. Aappropriate peroxidase-coupled secondary antibodies were applied for 1 hour at room temperature and peroxidase signals were detected using a chemiluminescent substrate (Pierce, Rockford, IL). Western blot analyses were run in triplicate.

Image processing and data analysis

Histological specimens were examined using an E-800 Nikon microscope (Nikon, Melville, NY) connected to a colour CCD Camera, a Leica TCS SP5 (Leica Microsystems, Wetzlar, Germany), or a Zeiss LSM710 (Carl Zeiss, Goettingen, Germany) confocal microscopes. All images were collected with the confocal microscope. Adobe Photoshop 6.0 (Adobe Systems, San Jose, CA) was used to adjust image contrast and assemble the final plates. Quantitative evaluations (cell densities, marker coexpression, soma diameters) were performed by confocal analysis or by means of the Neurolucida software (MicroBrightfield, Colchester, VT). Measurements derived from at least three sections per animal. Three to five animals were analysed for each time point or experimental condition. Routinely, a gray matter area (GM) of

about 500 μm^2 was evaluated together with the corresponding subcortical WM (see Supp. Info. Fig. 1B). WM was not analysed when confounding factors (i.e. proliferation of adjacent germinal areas; tightness of thin processes and high intensity of PLP/DM20 labelling) could affect the reliability of quantifications. For most markers, the number of inspected cells ranged from 100 to 700 cells per individual. In total, for BrdU (double pulse) and Ki67 staining at least 50-70 cells were analysed.

Soma diameters were calculated only for cells whose soma was entirely included in the confocal stack by averaging the values of their minimum and maximum diameters in two orthogonal directions (Kukley et al., 2010). Densitometric analysis of staining intensity and mapping of cell localization were made using ImageJ software (Research Service Branch, National Institutes of Health, Bethesda, MD; http://rsb.info.nih.gov/ij/). All quantifications were performed in the sensorimotor cortex (from -0.4 to -1.94 from bregma, Supp. Info. Fig. 1B). Statistical analyses were carried out by the SigmaStat software package (Jandel Scientific, Germany) and included one-way ANOVA test (to compare mean values) followed by Bonferroni's post-hoc analysis, unpaired Student's t test (when comparing only two groups), Fisher's exact text, Chi-square test or binomial test (to compare frequencies). Percentages were treated according to the arcsin transformation. In all instances, $P < 0.05$ was considered as statistically significant. Data were expressed as averages ± standard deviations.

RESULTS

Characterization of GPR17 expression in adult oligodendroglial cells

As an initial step of this study, we extended and detailed the first description of GPR17 expressing cells in the adult brain reported in Lecca et al. (2008). Consistent with these earlier findings, in the mature mouse cerebral cortex GPR17 antisera labelled some neurons (punctate somatic staining, arrows in Fig. 1D) and many other cells dispersed in the parenchyma. The non-neuronal cells were scattered in both GM (Fig. 1A) and WM (Fig. 1B) at a similar density (102.78 ± 26.18 cells/mm^2 and 114.18 ± 21.41 cells/mm^2 respectively, P=0.08) that remained quite stable over time during mouse ageing (cfr these data obtained in 2-4 month old animals and those for wild type mice in chronic amyloidosis analysis). Their oligodendroglial phenotype was confirmed by coexpression of the transcription factor Olig2 (see Supp. Info. Table 1, present in $93.57\pm3.44\%$ and $92.03\pm0.2\%$ of all GPR17+ cells in GM and WM, respectively; Fig. 1A-B'), and by the lack of costaining for microglial or astrocytic antigens (Iba1 and GFAP or S100β, respectively, data not shown). Furthermore, a careful confocal inspection revealed that in Olig2+ cells the GPR17 protein had distinct expression levels and cellular localisations. In about half of the cells ($56.8\pm5.6\%$ and $34.7\pm9.7\%$ in GM and WM, respectively), GPR17 protein was detected as a single intracellular spot (GPR17 protein, intracellular, henceforth mentioned as "Gpi" cells; arrows in Fig. 1A-B', C, arrowheads in Fig.1D,F',G; see also Lecca et al., 2008), corresponding mainly to the Golgi apparatus or also including the initial segments of 1-2 processes in tight contiguity with the Golgi pole (Fig. 1F,F'). Double staining analysis showed that these cells are distinct from GPR17-labelled neuron somata (Fig. 1D), and belong to multipolar oligodendrocyte precursors expressing NG2 (Stallcup, 2002) and PDGFRa (Nishiyama et al., 1996) (Fig.1C, G, L). NG2+ precursors displaying intracellular GPR17 protein were also found *in vitro* (Fig. 1E).

The rest of GPR17 positive cells exhibited a higher and broader GPR17 expression,

extended to both somata and processes and indicative of receptor localisation to the cell membrane (GPR17 receptor on cell membrane, henceforth mentioned as "Grm" cells; arrowheads in Fig. 1A-B'; H-K, M, N). Grm cells were proportionally more numerous among the GPR17+ population in the WM compared to GM (43.2±5.6% GM and 65.3±9.7 WM, $P<0.001$). Although lacking the precursor marker PDGFRa, about half of Grm cells still synthesised NG2 (Fig.1H-I', L: 46.62±22.90 % in GM; 43.82±9.09% in WM). As highlighted by detailed GM inspection, GPR17 labelling in processes was more prominent in cells with more complex morphologies (Fig. 1I) where, conversely, NG2 staining appeared reduced and discontinuous along ramifications, suggesting NG2 downregulation (Fig. 1H',I'). Interestingly, cells with highest receptor levels and broadest positive radiating processes were decorated for the immature proteolipid protein (PLP) splice variant PLP/DM20 (about 30% of Grm cells, GM; Kukley et al., 2010; Fig. 1J,L; and negative for the myelin protein PLP1, also detected by the AA3 antibody) and CD9 (Terada et al., 2002; Fig. 1K). Both PLP/DM20 and CD9 are well-known markers for premyelinating stages. Thus, Grm cells comprise both NG2+ elements and more mature premyelinating cells. This heterogeneity was also reflected in the range of cell soma sizes, comprising both small somata with diameters typical of PDGFRa precursors and a majority of larger cells with premyelinating features (Suppl. Fig. 2A,B; cfr also Kukley et al., 2010). Finally, Gpi and Grm cells together comprised about the 25% of the whole NG2+ cell population in both GM and WM (27.96 ± 7.59% and 22.3 ± 4.53%, respectively, $P=0.114$), demonstrating that GPR17 is translated in a relevant fraction of adult oligodendrocyte precursors. Accordingly, no colabelling was observed for GPR17 and markers for more mature or myelinating oligodendroglial stages such as glutathione S-transferase (GST)-π (Tamura et al., 2007; Fig. 1M), mature proteolipid protein (PLP1, Griffiths at al., 1998; Fig. 1N), 2',3'-cyclic nucleotide 3'-phosphodiesterase (RIP, Watanabe et al., 2006), myelin basic protein (MBP) and myelin

associated glycoprotein (MAG) (data not shown). On the whole, these data suggest that the Gpi and Grm staining patterns may represent different maturation stages of GPR17+ cells and that GPR17 can exert its receptor function in a fraction of adult NG2+ cells in transition to more mature stages and premyelinating oligodendrocytes.

GPR17 expression pattern during postnatal oligodendrocyte differentiation

With the aim to assess whether Gpi and Grm patterns constitute progressive phases of NG2+ cell maturation, we examined receptor expression during the first weeks of life. Similar to the adult brain, anti-GPR17 antibodies occasionally stained neurons (arrowheads in Fig. 2H, see also Fig. 3B and C) and clearly labelled Olig2+ cells (Fig. 2A-B'). The immunophenotype of these latter cells, as demonstrated by lack of coexpression of microglia- or astrocyte-specific markers (Iba1, GFAP, vimentin, data not shown), extensive overlap with NG2 (Fig. 2C), costaining for PDGFRa at low GPR17 expression levels (Fig. 2D), and absence of proteins typical for completed oligodendrocyte maturation (GST-π, PLP1, MAG and MBP, Fig. 2H-K), was consistent with that of adult GPR17+ cells.

GPR17+/Olig2+ cells were detected already at birth (Fig. 3A,E,F) and predominantly belonged to the Gpi type (Fig. 3A,H,I). During the first postnatal weeks, GPR17 expression was progressively increasing, as shown by the elevation in GPR17+ cell number between P0 and P7 (Fig. 3E,F) and by the enlargement of the Grm fraction, virtually absent at birth (Fig. 3H and I; P7-P14 vs. P0, $P<0.001$), indicating that the maturation of GPR17+ cells includes the switch from Gpi to Grm phenotypes. This interpretation was additionally strengthened by the observation that the distribution of GPR17 to cell ramifications recapitulated and anticipated the latero-medial and ventro-dorsal patterns of oligodendrocyte myelination in the cerebral cortex (Vincze et al., 2008; cfr Supp. Info. Fig. 3), although at earlier ages. Consistent with GPR17

upregulation during postnatal development, the fraction of GPR17 expressing cells among oligodendrocyte progenitors progressively increased (Fig.3G), and during the fourth postnatal week covered the vast majority of immature oligodendrocytes, identified either as Olig2+/Gst-π negative cells or as NG2+ cells (Fig. 3G, see also Fig. 4A). Interestingly, from P14, cells appeared that showed intense GPR17 positivity covering extended branches (Fig. 2E,G), as well as sparse processes aligning with axons or intercalating with the earliest myelin tracts (arrows in Fig. 2E,F,J,K), suggestive of premyelinating morphologies. Notably, these Grm cells often coexpressed PLP/DM20 and CD9 (Fig. 2E,G). Analysis of cortical GM at P24, showed that GPR17+/PLP/DM20+ cells covered about 60% of Grm cells (Fig. 4B). However, at this age NG2 was still coexpressed by the vast majority of GPR17+ cells, including both Gpi and Grm elements (Fig. 4A-B). These data imply some degree of overlap between NG2 and PLP/DM20 expression during postnatal differentiation (Fig. 4C, C'). Furthermore, in line with the adult phenotype and with different stages of maturation, Grm somata exhibited diameters typical of both oligodendrocyte precursors and premyelinating cells (Suppl. Info. Fig. 2).

Consistent with GPR17 anticipating myelination (see also Chen et al., 2009), massive myelin production followed the peak of GPR17+ cell density (P7-P14, Fig. 3A'-D' and Fig 3E, F) and occurred concomitantly with the decrease in GPR17+ cell number (Fig. 3D,D' and Fig. 3E,F). Western blot data confirmed these results (Fig. 3J). To explain the significant decrease in GPR17+ cell density in the progression to the mature stage (about 50% and 80% reduction in GM and WM, respectively; $P<0.05$, P24 vs. adult), possible signs of apoptosis in GPR17+ cells were evaluated by TUNEL assay and inspection of DAPI+ nuclei. Since we could not observe any positivity for DNA fragmentation or pyknosis (data not shown), the decline in GPR17+ cells is likely due to downregulation of the receptor during terminal differentiation. In summary, these data show that, similar to the adult pattern, GPR17 expression pertains to a fraction of postnatal

NG2+ cells in transition to maturity and that receptor expression is downregulated before the completion of myelin production.

Proliferative activity of GPR17-expressing cells in the adult and postnatal brain

One of the major and mostly debated traits of NG2+ cell heterogeneity is the capability to undergo cell proliferation (Bouslama-Oueghlani et al. 2005; Irvine and Blakemore, 2007; Rivers et al. 2008; Psachoulia et al., 2009; Simon et al., 2011). Considering the well-established role of GPR17 endogenous ligands (extracellular nucleotides, Ciana et al., 2006) as modulators of cell proliferation (Abbracchio et al., 1994; Agresti et al., 2005; Burnstock, 2006; Milosevic et al., 2006), we asked whether GPR17 expression could identify NG2+ cells endowed with a specific proliferative behaviour. To this aim, we applied diverse BrdU treatments to adult animals to analyse active mitosis (double pulse of the DNA base analogue BrdU followed by sacrifice, Suppl. Info Fig. 1A) or examine GPR17 + cell turnover (continuous administration of BrdU until sacrifice, Suppl. Info Fig. 1A) in comparison to NG2+ cells (see Material and Methods). In all cases, virtually all BrdU-incorporating cells were NG2+ (>80%).

When detecting cells undergoing or just exiting S-phase (BrdU double pulse protocol), only Gpi cells were decorated by BrdU staining while Grm cells were always negative (Fig. 5D,E). This observation was further confirmed by BrdU pulses at postnatal ages (P3, data not shown), and by labelling of the adult cortex for Ki67, a marker for active divisions (Taupin, 2007). The Gpi fractions among BrdU+ cells (22.35±7.45% in GM, 11.71±3.12% in WM, Fig. 5D,E) were overall in line with the corresponding Gpi proportions amongst NG2+ cells (19.31 ±5.6% in GM, 13.21±6.7% in WM; $P>0.05$). Consistently, the proliferative fractions of Gpi cells (2.27±1.29% in GM; 7.26±2.60% in WM) were similar to that of NG2+ cells (1.90±0.65% in GM; 8.36±2.00% in WM; $P>0.05$). Moreover, among Ki67+/NG2+ cells, 22.11±8.64% expressed the

GPR17 protein in the GM (Fig. 5D), while virtually none (1.13±2.27%) was positive in the WM (Fig. 5E). Thus, Gpi cells can undergo active proliferation and behave similarly to NG2+ precursors. The discrepancy between GM and WM highlighted also by the difference between the total number of BrdU+ and Ki67+ cells in these regions (Fig5 D, E), points to distinct cell cycle length and maturation speed in these territories (Dimou et al 2008; Kang et al 2010).

When long BrdU administration was applied, one day after starting the BrdU treatment, the proliferative proportion of GPR17-expressing cells was about 3 fold lower than that of NG2+ cells (Fig. 5A and B; $P<0.05$ in both GM and WM). Nevertheless, at later time points, this difference disappeared (Fig. 5A and B, $P>0.05$), thereby ruling out the possibility of a slower proliferation rate for the whole GPR17+ pool, and rather suggesting GPR17 upregulation over time in newly-generated cells. Notably, BrdU+/GPR17+ cells progressively increased in number and included the vast majority of GPR17+ cells within about one-month of treatment (14 days, GM, 31.33±8.72%, WM, 45.86±5.3%; 28 days, GM, 64.62±2.56%, WM, 77.14±12.06%), underlying that GPR17+ cells undergo a continuous turn over with rates similar to that of all NG2+ cells (present work and Simon et al., 2011). Furthermore, while at short times after cumulative BrdU treatment almost all GPR17+/BrdU+ cells belonged to the Gpi type (92.5±17.53% at 1 day), with longer exposures the receptor was also expressed in cell ramifications (Fig. 5F,L), consistent with a progressive upregulation of the receptor after division. In summary, GPR17 is induced in NG2+ cells by the end of the cell cycle and its upregulation defines a stage when cells are non-proliferative.

Timing and pattern of GPR17 induction in adult and postnatal newly generated NG2+ cells

Because the previous analysis suggested an upregulation of the receptor after proliferation, we performed BrdU-based label retaining experiments to examine the precise timing of GPR17 induction in newly generated NG2+ cells. In a first set of experiments, a synchronized pool of newborn cells labelled by a double BrdU pulse (Supp. Info. Fig. 1A) was followed over time. The fractions of GPR17+/BrdU+ cells expanded to about half of all newborn cells by 4-7 dpi (4dpi 56.69±8.73% and 36.96±5.09%, 7dpi 52.01±2.46% and 39.14±4.59% in GM and WM, respectively, Fig. 5H and I) but never covered the entire BrdU-tagged population. In both GM and WM, the double-positive fractions declined at later time points and WM cells exhibited a faster kinetic (about 45% decline between 4 and 7dpi vs. 60% decline in GM only after 7dpi). In WM this reduction was accompanied by a decrease in the absolute number of BrdU+ cells, again suggesting a major propensity of WM cells to undergo multiple divisions and therefore to dilute out the incorporated BrdU (Dimou et al., 2008; Kang et al. 2010). In agreement with the pattern of postnatal ontogenesis, while at 1 dpi virtually all the newly generated GPR17+ cells were Gpi, at 4 and 7 dpi Grm cells with strong and spread receptor expression covered a relevant fraction (4 dpi, 35.26±5.7% and 57.41±15.3%; 7 dpi, 32.78±7.52% and 57.78±6.71% in GM and WM, respectively). Further on, the Grm proportions diminished again (13.03±10.57% and 23.81±13.47% in GM and WM, respectively), confirming the transient expression of the receptor and the maintenance of GPR17 for long times only in a small cell pool. Similar data were also obtained when GPR17 regulation was examined in newly produced oligodendrocyte precursor of the immature cortex (Supp. Info. Fig. 4). Again, GPR17 did not appear in all GM BrdU+ cells, and was transiently regulated.

The BrdU treatment employed so far labelled cells capable of DNA duplication within few hours (fast dividing cells) that appeared rather rare in the adult parenchyma (Fig. 5D,E). Nonetheless, adult NG2+ cells likely comprise cells with longer cell cycle lengths. To include

these cells, we tagged both fast and slow proliferating cells by administering BrdU for two weeks (Supp. Info. Fig 1A) and evaluated the fate of BrdU-incorporating cells (virtually all were NG2+, see Simon et al., 2011) in terms of GPR17 expression at the end of treatment and up to 10 weeks after. While the total number of GPR17+ cells remained stable over time (not shown, see also above), GPR17+/BrdU+ cells increased during the first 2 weeks of retaining in the GM (Fig. 5J,K), further supporting the hypothesis that the receptor is induced after proliferation. In the WM, this early induction was not appreciable, likely because it was masked by both a fast receptor decline and a prompt differentiation to mature oligodendrocytes (see double BrdU pulse data and below). The double+ cells were then decreasing in both GM and WM (see also Fig. 5F,G and L, M), consistent with progression to differentiation. Interestingly, and in agreement with previous data, in the WM the decline in the number of double+ cells after 2 weeks retaining was more pronounced compared to GM (Fig. 5J,K and F,G,L,M), supporting the notion of distinct differentiation properties of GM and WM NG2+ cells (Dimou et al., 2008; Kang et al., 2010). In addition, and in agreement with the short BrdU pulse data, the fraction of double+ cells among all BrdU+ cells never reached 100% in both GM and WM (Fig. 5J and K).

On the whole, these data indicate that GPR17 upregulation occurs early after mitosis and that, within the time limits of our analysis, pertains only to a subset of NG2+ cells. Furthermore, they show that GPR17 expression is transitory, and that receptor expression is regulated according to distinct kinetics in GM and WM.

GPR17+ cells participate in the parenchymal response to traumatic injury

The emerging role of endogenous nucleotides as danger signals upon brain and spinal cord injury (Wang et al., 2004; Davalos et al., 2005; Haynes et al., 2006), has raised the hypothesis that GPR17 responding to extracellular nucleotides and cysteinyl-leukotrienes may act as a

crucial mediator of NG2+ cell reactivity (Hampton et al., 2004, Simon et al., 2011) to acute injury such as cortical trauma (stab-wound, SW).

After SW, GPR17+ cells maintained their phenotype as shown by Olig2 and NG2 coexpression and absence of mature oligodendroglial markers or GFAP costaining (data not shown). At variance with what occurred in other CNS injury models (Lecca et al., 2008; Ceruti et al., 2009), after SW GPR17 was neither detected in Iba1+ microglial cells nor was found in round-shaped NG2+ blood-derived macrophages (data not shown, see Hampton et al., 2004) or in NG2+ pericytes. At 1 day post lesion (dpl) the density of GM GPR17+ oligodendroglial cells was reduced to one fourth of the value of the contralateral cortex (Fig. 6B,E; $P<0.05$), which was similar to that of intact mice ($P>0.05$). This decrease was accompanied by significant reduction in the Grm proportion (Fig. 6F, about 30% less than controls; $P<0.01$), and the GPR17 fraction amongst NG2+ cells (7.97±0.96 %; $P<0.001$), whose density was unchanged (Fig. 6E). Conversely, the density of GPR17+ cells did not change shortly after lesion in the WM (Fig. 6H), once more underlying distinct properties of GM/WM cells. At later time points, GPR17+ cells increased significantly in number around the lesion in both GM and WM, consistently with the expansion of NG2+ pool (Fig. 6C, E, H). This reactivity lasted up to 7 days and then declined over time, going back to basal levels at 14 dpl, when, conversely, NG2+ cell density was still increased (Fig. 6E and H). The time-dependent pattern of receptor expression revealed by immunohistochemical analysis was confirmed by quantitative evaluation of GPR17 mRNA in the lesioned cortex (Supp. Info Fig. 5A).

To substantiate the evidence for a post-acute GPR17 upregulation after SW, we found that the GM Grm fraction significantly exceeded control values between 4 and 14 dpl (Fig. 6F; $P<0.001$). Conversely, this did not occur in the WM (Fig. 6I). Interestingly, the pattern of Grm expansion displayed a specific spatio-temporal distribution: while Gpi cells increased in density

close to the lesion site at 4 dpl, Grm cells remained mostly located far away from the lesion (250-300 μm) and appeared closer to the SW only at later time points (Supp. Info Fig. 6). This observation likely reflects a distal-to proximal wave of NG2+ cell maturation.

Finally, we assessed whether GPR17+ cells, although being reduced in number early after lesion, might specifically contribute to NG2+ cell reactivity with intense proliferative activity. At short times after BrdU administration, dividing GPR17+ cells exclusively belonged to the Gpi type, as also observed in the intact brain. Moreover, at 1 day after BrdU cumulative treatment (dpt) the GPR17+ proliferative fraction remained lower than that of NG2+ cells (Fig. 6G; P=0.028) in GM, while in WM it reached the levels of NG2+ cells (Fig. 6J; P>0.05). Afterwards, as it was the case in the intact cortex, BrdU incorporation into GPR17+ and NG2+ cells was almost equivalent (P>0.05), showing that about 80% of both cell types had been generated "de novo" over the examined time window (Fig. 6G and J). Thus, the presence of GPR17 does not define a NG2+ cell subset capable to trigger and sustain NG2+ cell reaction to acute lesion by GPR17 upregulation or proliferation. Rather, receptor induction takes part in the post-acute response to damage according to a pattern reminiscent of GPR17 expression during oligodendroglia ontogenesis.

GPR17+ cells participate in the parenchymal response to chronic amyloidosis

To study the possible contribution of GPR17 expressing cells to the parenchymal response to a chronic injury, we investigated its expression in the APPPS1 mouse, a transgenic model of Alzheimer's Disease (Buffo et al., 2005; Radde et al., 2006). Also in this lesion condition, GPR17 staining was never observed in GFAP+ astrocytes (data not shown), Iba1+ microglial cells, or in mature oligodendrocytes (data not shown). Notably, GPR17+/Olig2+ cells increased significantly in number in the APPPS1 cortical GM (Fig. 7B and C; P<0.05) compared to age-

matched WT animals. However, the fraction of GM NG2+ cells coexpressing the receptor in APPPS1 cortices (28.17±2.85%) remained similar to that of WT mice (29.76±5.79%). On the contrary, GPR17+ cell density was unchanged in the underlying WM (123.34±10.55 cells/mm^2 APPPS1; 128.72±27.08 cells/mm^2 WT), where β-amyloid plaques are less abundant, indicating a specific correlation between amyloid aggregates and the increase in the GPR17+ cell number. In the GM most GPR17+ cells (64.51±4.01%) clustered in close proximity of β-amyloid plaques (within 50 μm from the plaque border; Fig. 7B,B'), where also Iba1+ microglial cells accumulated (Fig. 7B'). Here, the majority of GPR17+ cells (74.39±13.28% vs. 43.2±5.6% of controls, P<0.001) displayed a strong receptor labelling along the whole cell body and processes (Grm type; Fig. 7D), further supporting the correlation between GPR17 induction and plaques. Yet, no significant upregulation of the GPR17 mRNA content was found in APPPS1 cortex (Supp. Info Fig. 5B), suggesting a modulation at the level of translation or of the stability of GPR17 protein.

When proliferation of GPR17+ cells was analysed after a 7 day-long administration of BrdU (Fig. 7E), we found a distinct behaviour for GPR17+ and NG2+ cells in the APPPS1 cortical GM. While the NG2+ cell population maintained its rate of division, the fraction of BrdU-labelled GPR17 expressing cells was significantly higher in the APPPS1 cortex than that in wild type mice (Fig. 7E; P<0.001). However, even in this condition, actively dividing cells labelled by means of two subsequent BrdU injections belonged to the Gpi type, whereas Grm cells never incorporated BrdU (not shown). Moreover, the proliferative fraction of GPR17 expressing cells remained similar to that of wild type animals (1.52±0.77% in APPPS1, 1.28±0.72% in WT, after a double BrdU pulse). Thus, the increase in the GPR17+ proliferative fraction, rather than reflecting an enhanced active proliferation, is consistent with an anticipated induction of the receptor in newly generated cells and/or with its maintenance for longer times. On the whole, these data reveal that the upregulation of GPR17 is a hallmark of reactivity to cerebral

amyloidosis.

DISCUSSION

To shed light on the heterogeneity and antigenic indistinguishability of NG2+ cells, we examined the expression pattern of the newly identified oligodendroglial GPR17 receptor in the intact mouse cerebral cortex at mature and developmental stages, and in conditions of traumatic injury and chronic amyloidosis. We show that in the adult and early postnatal cortex NG2+ cells progressively upregulate GPR17 after cell division until they reach the premyelinating stage. GPR17 downregulation, occurring with distinct kinetics in gray and white matter, coincides with further differentiation of cells and expression of myelin proteins (Table 1). During postnatal ontogenesis, GPR17 appearance anticipates the major myelination phase and decorates a proportion of oligodendroglial precursors initially expanding within the first month of life, and then decreasing as the tissue matures. GPR17 induction also participates in the response to traumatic injuries at post-acute stages and to chronic pathology.

GPR17 in NG2+ cell diversity and maturation

NG2-expressing cells display heterogeneous functional and phenotypical characteristics in distinct CNS territories, upon lesion or during ageing (Gilson and Blakemore, 1993; Levine et al., 1993; Hampton et al., 2004; Dimou et al., 2008; Rivers et al., 2008; Irvine and Blakemore, 2007; Simon et al., 2011). While both extrinsic environmental cues and intrinsic factors have been proposed to explain such variability (Hampton et al, 2004; Dimou et al., 2008; Lytle et al., 2009; Nishiyama et al, 2009), the molecular substrates discriminating specific functional competences or distinct maturation stages among NG2+ cells remain essentially unidentified. Our study reveals that diverse GPR17 expression levels and compartmentalization identify

defined oligodendroglial statuses. Indeed, low expression and intracellular localisation of GPR17 protein, indicative of the early activation of its biosynthetic pathway, correspond to NG2+ cells in mitosis, or that just exited mitosis. Conversely, high GPR17 levels in both perikarium and processes and its localisation on the cell membrane define a more mature and non-proliferative stage of oligodendroglial cells. Further, intense GPR17 expression accompanies these cells until the premyelinating stage. On the whole, these results point to GPR17 induction as a marker of maturation of NG2+ cells in transition from precursor to premyelinating phenotypes. These data also suggest that the GPR17 receptor exerts its function of detector of extrinsic signals in post-mitotic NG2+ cells and premyelinating oligodendrocytes, and clarify that, given its intracellular localisation, it cannot act in that way in proliferative NG2+/PDGFRa+ precursors.

Notably, however, GPR17 induction characterizes only about one third of the progeny of the cycling NG2+ pool, meaning that that diverse progenitor subsets exist with distinct molecular mechanisms to sense the environment and regulate their fate. While intracellular GRP17 protein does not confer specific proliferative capabilities to NG2+ cells, exposure of the receptor to the cell membrane coincides with non-mitotic stages, in line with their commitment to differentiation. This finding suggests that receptor positive and negative progenies may have diverse differentiation capabilities. GPR17-mediated signals have been proposed to be required for receptor downregulation and further cell maturation (Lecca et al., 2008; Fumagalli et al., 2011; E. Parmigiani et al., unpublished). Our *in vivo* data on receptor downregulation before expression of myelin proteins are in line with these results and also highlight a function of GPR17 in the acquisition of premyelinating traits. Nevertheless, while we clearly proved that GPR17 expressing cells are engaged in differentiation (at least until the premyelinating stage), we have no elements to infer whether receptor negative NG2+ cells remain immature or

differentiate. The early appearance of mature and myelinating oligodendrocytes in the first weeks of postnatal life, occurring well before the decrease in GPR17+ cell numbers (Fig. 3E,F), suggests that receptor negative cells are also able to progress to differentiation. However, the broader GPR17 distribution to cell processes in the adult WM compared to GM and the faster receptor downregulation in WM cells compared to GM ones well correlate with more efficient myelination capabilities in this territory (Dimou et al., 2008), consistently with GPR17 induction, signalling and downregulation being crucial for maturation of NG2+ cells to oligodendrocytes (Lecca et al., 2008; Chen et al., 2009; Fumagalli et al., 2011). Yet, only cell tracking experiments of GPR17-positive/negative cells will resolve the issue of distinct differentiation capabilities of negative and positive pools. Similarly, only pharmacological studies with GPR17-selective compounds in native systems will disclose the exact mechanisms of GPR17 functioning.

Regulation of GPR17 expression

The existence of GPR17-positive and negative NG2+ cells brings up the issues of the lineage relationships between these cell subsets and of the mechanisms regulating GPR17 expression. The finding that GPR17+/NG2+ cells can derive from receptor-negative mitotic cells suggests that the two subsets do not belong to separate clones. Moreover, the correspondence between the timing of GPR17 appearance during postnatal development and the pattern of oligodendrocyte maturation strongly points to the existence of an intrinsic activation program for GPR17 expression, appearing thus as a default event, at least in the lineage of an oligodendrocyte subset. Distinct progenitor populations originating either in the ventral or dorsal forebrain ventricular zones have been described to contribute to embryonic, postnatal and adult cortical oligodendroglia (Kessaris et al., 2006). Whether intrinsic

determinants encoded in these forebrain progenitor populations account for receptor-positive and -negative pools is not known. Despite ventral and dorsal oligodendroglia cells have been shown to share several features (electrical properties, number of wrapped axons, neurotransmitter receptor responses, Tripathi et al., 2011), in future studies it will be interesting to examine whether GPR17 differentially pertains to these populations. However, Lecca and coworkers (2008) also demonstrated that, besides stimulating differentiation, GPR17 endogenous ligands also directly affect GPR17 expression, thus pointing to an extrinsic time- and regional-specific activation program for receptor induction. Indeed, uracyl nucleotides and their glycosylated derivatives are released not only in lesion conditions but also in the intact parenchyma (Lecca and Ceruti 2008), therefore potentially contributing to GPR17 physiological regulation. Our study further suggests that signals associated to β-amyloid plaques participate in inducing and/or maintaining high levels of receptor expression. Such signals may derive from dystrophic (Wirths et al., 2007), demyelinated or dysmyelinated axons (Desai et al., 2009; G. Behrendt, unpublished) and/or from activated microglia (Radde et al., 2006). Similarly, signals acutely released at the site of traumatic lesion modulate GPR17 synthesis. In fact, early after stab-wound receptor expression is downregulated in NG2+ cells. Notably, such changes do not occur in the damaged WM, underscoring once again the different features of gray and white matter territories. Growth factors appear as possible candidates for GM downregulation, because they take part in the tissue reaction to injury (Buffo et al., 2010) and have been shown to dampen GPR17 expression in oligodendrocyte precursors *in vitro* (Ceruti et al., 2011).

GPR17 expressing cells in injury

While former reports indicated that receptor activity mediates acute neuronal and myelin vulnerability to ischemic and traumatic injury (Ciana et al., 2006, Lecca et al, 2008; Ceruti et al., 2009), here we clarify that GPR17 neither is upregulated in NG2+ progenitors as part of their early reactivity, nor receptor activity triggers an increased proliferative response in positive cells. Conversely, GPR17 induction takes place at post-acute stages of tissue remodelling and recapitulates the ontogenetic pattern of receptor expression. In agreement with these data, GPR17+ cells do not activate rapid proliferation in chronic cerebral amyloidosis and accumulate close to plaques, revealing receptor induction as an additional feature of oligodendroglial reactivity in this pathology (Buffo et al., 2005). Our data indicate that the timing of GPR17 appearance in oligodendrocyte progenitors reacting to lesion likely reflects newborn cell maturation, and may correlate with regenerative attempts directed at repairing oligodendrocyte damage occurring under these injury conditions (Lotocki et al., 2011; Mitew et al., 2010; Desai et al., 2009). However, receptor overexpression was also described in an immune-mediated model of chronic demyelination, where recurrent myelin damage is not compensated by NG2+ cell reparative responses, supporting the interpretation of GPR17 as a factor hampering of myelin restoration (Chen at al., 2009). Yet, we found a strong GPR17 induction in a focal demyelination model (Supp. Info Fig. 7), where spontaneous recovery normally occurs (Woodruff and Franklin, 1999; Birgbauer et al., 2004). Notably, also in this case GPR17+ cells accrued at sites of demyelination at post-acute stages, in a time window corresponding to the initiation of oligodendrocyte repair (Woodruff and Franklin, 1999). These data would rather support a function for the receptor in myelin reconstitution. To tentatively reconcile these different interpretations, it may be hypothesized that GPR17 induction reflects an initial attempt to start re-myelination, but that its dysregulated sustained over-expression at late oligodendroglial maturation stages as a result of the local inflammatory microenvironment

turns an initial beneficial reaction into a detrimental one. Thus, given the massive presence of GPR17 in oligodendrocyte progenitors during post-acute reactivity to various injury conditions, with diverse extent of oligodendrocyte damage and reparative outcomes, it will be crucial to understand whether and how manipulations of GPR17 may potentiate reparative myelination.

Acknowledgments

References

Abbracchio MP, Saffrey MJ, Höpker V, Burnstock G.1994. Modulation of astroglial cell proliferation by analogues of adenosine and ATP in primary cultures of rat striatum. Neuroscience 59:67-76.

Agresti C, Meomartini ME, Amadio S, Ambrosini E, Serafini B, Franchini L, Volonte C, Aloisi F, Visentin S. 2005. Metabotropic P2 receptor activation regulates oligodendrocyte progenitor migration and development. Glia 50:132-144.

Bakiri Y, Attwell D, Karadottir R. 2009. Electrical signalling properties of oligodendrocyte precursor cells. Neuron Glia Biol 5:3-11.

Birgbauer E, Rao TS, Webb M. 2004. Lysolecithin induces demyelination in vitro in a cerebellar slice culture system. J Neurosci Res 78:157-166.

Boda E, Buffo A. 2010. Glial cells in non-germinal territories: insights into their stem/progenitor properties in the intact and injured nervous tissue. Arch Ital Biol 148:119-136.

Boda E, Pini A, Hoxha E, Parolisi R, Tempia F. 2009. Selection of reference genes for quantitative real-time RT-PCR studies in mouse brain. J Mol Neurosci 37:238-253.

Bouslama-Oueghlani L, Wehrle R, Sotelo C, Dusart I. 2005. Heterogeneity of NG2-expressing cells in the newborn mouse cerebellum. Dev Biol 285:409-421.

Buffo A, Rolando C, Ceruti S. 2010. Astrocytes in the damaged brain: molecular and cellular insights into their reactive response and healing potential. Biochem Pharmacol 79:77-89.

Buffo A, Vosko MR, Erturk D, Hamann GF, Jucker M, Rowitch D, Gotz M. 2005. Expression pattern of the transcription factor Olig2 in response to brain injuries: implications for neuronal repair. Proc Natl Acad Sci U S A 102:18183-18188.

Burnstock G. 2006. Purinergic signalling. Br J Pharmacol 147 Suppl 1:S172-181.

Butt AM, Kiff J, Hubbard P, Berry M. 2002. Synantocytes: new functions for novel NG2

expressing glia. J Neurocytol 31:551-565.

Ceruti S, Villa G, Genovese T, Mazzon E, Longhi R, Rosa P, Bramanti P, Cuzzocrea S, Abbracchio MP. 2009. The P2Y-like receptor GPR17 as a sensor of damage and a new potential target in spinal cord injury. Brain 132:2206-2218.

Ceruti S, Viganò F, Boda E, Ferrario S, Magni G, Rosa P, Buffo A, Abbracchio MP. 2011. Expression of the new P2Y-like receptor GPR17 during oligodendrocyte precursor cell maturation regulates sensitivity to ATP-induced death. Glia 59: 363-378.

Chen Y, Wu H, Wang S, Koito H, Li J, Ye F, Hoang J, Escobar SS, Gow A, Arnett HA, Trapp BD, Karandikar NJ, Hsieh J, Lu QR. 2009. The oligodendrocyte-specific G protein-coupled receptor GPR17 is a cell-intrinsic timer of myelination. Nat Neurosci 12:1398-1406.

Ciana P, Fumagalli M, Trincavelli ML, Verderio C, Rosa P, Lecca D, Ferrario S, Parravicini C, Capra V, Gelosa P, Guerrini U, Belcredito S, Cimino M, Sironi L, Tremoli E, Rovati GE, Martini C, Abbracchio MP. 2006. The orphan receptor GPR17 identified as a new dual uracil nucleotides/cysteinyl-leukotrienes receptor. EMBO J 25:4615-4627.

Ciceri P, Rabuffetti M, Monopoli A, Nicosia S. 2001. Production of leukotrienes in a model of focal cerebral ischaemia in the rat. Br J Pharmacol 133:1323-1329.

Davalos D, Grutzendler J, Yang G, Kim JV, Zuo Y, Jung S, Littman DR, Dustin ML, Gan WB. 2005. ATP mediates rapid microglial response to local brain injury in vivo. Nat Neurosci 8:752-758.

Dawson MR, Polito A, Levine JM, Reynolds R. 2003. NG2-expressing glial progenitor cells: an abundant and widespread population of cycling cells in the adult rat CNS. Mol Cell Neurosci. 24:476-88.

De Biase LM, Nishiyama A, Bergles DE. 2010. Excitability and synaptic communication within the oligodendrocyte lineage. J Neurosci 30:3600-3611.

Desai MK, Sudol KL, Janelsins MC, Mastrangelo MA, Frazer ME, Bowers WJ. 2009. Triple-transgenic Alzheimer's disease mice exhibit region-specific abnormalities. Glia 57:54-65.

Dimou L, Simon C, Kirchhoff F, Takebayashi H, Gotz M. 2008. Progeny of Olig2-expressing progenitors in the gray and white matter of the adult mouse cerebral cortex. J Neurosci 28:10434-10442.

Fumagalli M, Daniele S, Lecca D, Lee PR, Parravicini C, Fields RD, Rosa P, Antonucci F, Verderio C, Trincavelli ML, Bramanti P, Martini C, Abbracchio MP. 2011. Phenotypic changes, signaling pathway, and functional correlates of GPR17-expressing neural precursor cells during oligodendrocyte differentiation. J Biol Chem 286:10593-10604.

Gilson J, Blakemore WF. 1993. Failure of remyelination in areas of demyelination produced in the spinal cord of old rats. Neuropathol Appl Neurobiol 19:173-181.

Griffiths I, Klugmann M, Anderson T, Thomson C, Vouyiouklis D, Nave KA. 1998 Current concepts of PLP and its role in the nervous system. Microsc Res Tech 41:344-358.

Hampton DW, Rhodes KE, Zhao C, Franklin RJ, Fawcett JW. 2004. The responses of oligodendrocyte precursor cells, astrocytes and microglia to a cortical stab injury, in the brain. Neuroscience 127:813-820.

Haynes SE, Hollopeter G, Yang G, Kurpius D, Dailey ME, Gan WB, Julius D. 2006. The P2Y12 receptor regulates microglial activation by extracellular nucleotides. Nat Neurosci 9:1512-1519.

Horner PJ, Power AE, Kempermann G, Kuhn HG, Palmer TD, Winkler J, Thal LJ, Gage FH. 2000. Proliferation and differentiation of progenitor cells throughout the intact adult rat spinal cord. J Neurosci 20:2218-2228.

Irvine KA, Blakemore WF. 2007. A different regional response by mouse oligodendrocyte progenitor cells (OPCs) to high-dose X-irradiation has consequences for repopulating OPC-

depleted normal tissue. Eur J Neurosci 25:417-424.

Jung M, Kramer E, Grzenkowski M, Tang K, Blakemore W, Aguzzi A, Khazaie K, Chlichlia K, von Blankenfeld G, Kettenmann H, et al. 1995. Lines of murine oligodendroglial precursor cells immortalized by an activated neu tyrosine kinase show distinct degrees of interaction with axons in vitro and in vivo. Eur J Neurosci 7:1245-1265.

Kang SH, Fukaya M, Yang JK, Rothstein JD, Bergles DE. 2010. NG2+ CNS glial progenitors remain committed to the oligodendrocyte lineage in postnatal life and following neurodegeneration. Neuron 68:668-81.

Kessaris N, Fogarty M, Iannarelli P, Grist M, Wegner M, Richardson WD. 2006. Competing waves of oligodendrocytes in the forebrain and postnatal elimination of an embryonic lineage. Nat Neurosci 9:173-179.

Kukley M, Nishiyama A, Dietrich D. 2010. The fate of synaptic input to NG2 glial cells: neurons specifically downregulate transmitter release onto differentiating oligodendroglial cells. J Neurosci 30:8320-8331.

Lecca D, Ceruti S. 2008. Uracil nucleotides: from metabolic intermediates to neuroprotection and neuroinflammation. Biochem Pharmacol 75:1869-1881.

Lecca D, Trincavelli ML, Gelosa P, Sironi L, Ciana P, Fumagalli M, Villa G, Verderio C, Grumelli C, Guerrini U, Tremoli E, Rosa P, Cuboni S, Martini C, Buffo A, Cimino M, Abbracchio MP. 2008. The recently identified P2Y-like receptor GPR17 is a sensor of brain damage and a new target for brain repair. PLoS One 3:e3579.

Levine JM, Stincone F, Lee YS. 1993. Development and differentiation of glial precursor cells in the rat cerebellum. Glia 7:307-321.

Livak KJ, Schmittgen TD. 2001. Analysis of relative gene expression data using real-time quantitative PCR and the 2(-Delta Delta C(T)) Method. Methods 25:402-408.

Lotocki G, Vaccari, Jde R, Alonso O, Molano JS, Nixon R, Safavi P, Dietrich WD, Bramlett HM. 2011 Oligodendrocyte vulnerability following traumatic brain injury in rats. Neurosci Lett. 499:143-148.

Lytle JM, Chittajallu R, Wrathall JR, Gallo V. 2009. NG2 cell response in the CNP-EGFP mouse after contusive spinal cord injury. Glia 57:270-285.

Melani A, Turchi D, Vannucchi MG, Cipriani S, Gianfriddo M, Pedata F. 2005. ATP extracellular concentrations are increased in the rat striatum during in vivo ischemia. Neurochem Int 47:442-448.

Milosevic J, Brandt A, Roemuss U, Arnold A, Wegner F, Schwarz SC, Storch A, Zimmermann H, Schwarz J. 2006. Uracil nucleotides stimulate human neural precursor cell proliferation and dopaminergic differentiation: involvement of MEK/ERK signalling. J Neurochem 99:913-923.

Mitew S, Kirkcaldie MT, Shepard CE, Vickers JC, Dickson TC. 2010 Focal demyelination in Alzheimer's disease and transgenic mouse models. Acta Neuropathol. 119:567-577.

Nishiyama A, Lin XH, Giese N, Heldin CH, Stallcup WB. 1996. Co-localization of NG2 proteoglycan and PDGF alpha-receptor on O2A progenitor cells in the developing rat brain. J Neurosci Res 43:299-314.

Nishiyama A, Watanabe M, Yang Z, Bu J. 2002. Identity, distribution, and development of polydendrocytes: NG2-expressing glial cells. J Neurocytol 31:437-455.

Nishiyama A, Komitova M, Suzuki R, Zhu X. 2009. Polydendrocytes (NG2 cells): multifunctional cells with lineage plasticity. Nat Rev Neurosci 10:9-22.

Psachoulia K, Jamen F, Young KM, Richardson WD. 2009. Cell cycle dynamics of NG2 cells in the postnatal and ageing brain. Neuron Glia Biol 5:57-67.

Pugliese AM, Trincavelli ML, Lecca D, Coppi E, Fumagalli M, Ferrario S, Failli P, Daniele S,

Martini C, Pedata F, Abbracchio MP. 2009. Functional characterization of two isoforms of the P2Y-like receptor GPR17: [35S]GTPgammaS binding and electrophysiological studies in 1321N1 cells. Am J Physiol Cell Physiol 297:C1028-1040.

Radde R, Bolmont T, Kaeser SA, Coomaraswamy J, Lindau D, Stoltze L, Calhoun ME, Jaggi F, Wolburg H, Gengler S, Haass C, Ghetti B, Czech C, Holscher C, Mathews PM, Jucker M. 2006. Abeta42-driven cerebral amyloidosis in transgenic mice reveals early and robust pathology. EMBO Rep 7:940-946.

Rivers LE, Young KM, Rizzi M, Jamen F, Psachoulia K, Wade A, Kessaris N, Richardson WD. 2008. PDGFRA/NG2 glia generate myelinating oligodendrocytes and piriform projection neurons in adult mice. Nat Neurosci 11:1392-1401.

Simon C, Götz M, Dimou L. (2011) Progenitors in the adult cerebral cortex: Cell cycle properties and regulation by physiological stimuli and injury. Glia 59:869-881. Stallcup WB. 2002. The NG2 proteoglycan: past insights and future prospects. J Neurocytol 31:423-435.

Tamura Y, Kataoka Y, Cui Y, Takamori Y, Watanabe Y, Yamada H. 2007. Intracellular translocation of glutathione S-transferase pi during oligodendrocyte differentiation in adult rat cerebral cortex in vivo. Neuroscience 148:535-540.

Taupin P. 2007. BrdU immunohistochemistry for studying adult neurogenesis: paradigms, pitfalls, limitations, and validation. Brain Res Rev. 53:198-214.

Taverna E, Saba E, Rowe J, Francolini M, Clementi F, Rosa P. 2004. Role of lipid microdomains in P/Q-type calcium channel (Cav2.1) clustering and function in presynaptic membranes. J Biol Chem 279:5127-5134.Terada N, Baracskay K, Kinter M, Melrose S, Brophy PJ, Boucheix C, Bjartmar C, Kidd G, Trapp BD. 2002. The tetraspanin protein, CD9, is expressed by progenitor cells committed to oligodendrogenesis and is linked to beta1 integrin, CD81, and Tspan-2. Glia 40:350-359.

Tripathi RB, Clarke LE, Burzomato V, Kessaris N, Anderson PN, Attwell D and William D. Richardson WD. 2011. Dorsally and Ventrally Derived Oligodendrocytes Have Similar Electrical Properties but Myelinate Preferred Tracts J Neurosci 31:6809–6819.

Trotter J, Karram K, Nishiyama A. 2010. NG2 cells: Properties, progeny and origin. Brain Res Rev 63:72-82.

Vincze A, Mazlo M, Seress L, Komoly S, Abraham H. 2008. A correlative light and electron microscopic study of postnatal myelination in the murine corpus callosum. Int J Dev Neurosci 26:575-584.

Wang X, Arcuino G, Takano T, Lin J, Peng WG, Wan P, Li P, Xu Q, Liu QS, Goldman SA, Nedergaard M. 2004. P2X7 receptor inhibition improves recovery after spinal cord injury. Nat Med 10:821-827.

Watanabe M, Sakurai Y, Ichinose T, Aikawa Y, Kotani M, Itoh K. 2006. Monoclonal antibody Rip specifically recognizes 2',3'-cyclic nucleotide 3'-phosphodiesterase in oligodendrocytes. J Neurosci Res 84:525-533.

Wirths O, Weis J, Kayed R, Saido TC, Bayer TA. 2007. Age-dependent axonal degeneration in an Alzheimer mouse model. Neurobiol Aging 28:1689-1699.

Woodruff RH, Franklin RJ. 1999. Demyelination and remyelination of the caudal cerebellar peduncle of adult rats following stereotaxic injections of lysolecithin, ethidium bromide, and complement/anti-galactocerebroside: a comparative study. Glia 25:216-228.

Figure legends

Figure 1. Phenotype of GPR17-expressing cells in the adult cortex. A-B': in the intact cortex, cells with either intracellular (Gpi type, arrows) or radiate (Grm type, arrowheads) GPR17 staining displayed Olig2 positivity in both gray (A,A') and white matter (B,B'). However, GPR17+/Olig2+ cells represented only a fraction of all Olig2+ cells (A,B). C,E, C-G: intracellular GPR17 spots belonged to NG2- (red in C, single confocal plane, and E, cell in vitro) and PDGFRa- (red in G, single confocal plane) expressing cells while diffuse somatic punctate staining corresponded to neurons (D). It often localized to the Golgi apparatus (red in F, immunostained with anti-GS28 antibody) or included also the starting segments of 1 or 2 cell processes (arrowhead in F'). H-I': NG2 positive Grm cells (labelled by anti-AN2 antibody) with distinct morphologies and receptor expression levels. J-K: Grm cells with intense receptor staining and broad radiating processes express premyelination markers. M,N: no colocalisation was found between GPR17 and markers for mature oligodendrocytes, such as GST-π (M) and PLP1 (N). Micrographs are confocal stacks comprising 15-20 optical sections 1mm thick. Somatic yellow pixels in J,K resulted from the overlapping of distinct optical images. L: quantifications of fractions of double positive cells over the GPR17 expressing subsets. DAPI (blue) counterstains nuclei. The dotted line in (B) indicates the boundary between gray and white matter. GM, gray matter; WM, white matter; Gpi, intracellular GPR17 protein; Grm, GPR17 receptor on cell membrane. Scale bars: 50 µm in A, B; 10 µm in B'-K; 20 µm in A', M, N.

Figure 2. Phenotype of GPR17-expressing cells during postnatal development. A-B': GPR17

is expressed in a subset of Olig2+ cells in the immature cerebral cortex. Both Grm (B) and Gpi (B') cell types were present among postnatal GPR17+ cells. C: virtually all GPR17+ cells coexpressed NG2. D: cells with intracellular GPR17 protein exhibited PDGFRa positivity. E, G: cells with high levels of receptor expression were stained also by anti PLP/DM20 (E, E') or CD9 (G, G') antibodies. H-K: no colocalisation was found with markers for mature oligodendrocytes, such as GST-π (H), PLP1 (I), MAG (J) and MBP (K). Some GPR17 processes run in parallel and intercalated with SMI32+ axons (F, F') and myelin tracts (J-K'). Micrographs are confocal stacks comprising 15-20 optical sections 1μm thick. Yellow pixels in H-J resulted from the overlapping of distinct optical images. No marker colocalisation was found in single optical sections. All micrographs are obtained from P14 cortex, with the exception of (C) obtained from a P7 brain. Arrowheads in (H) indicate neurons labelled by anti-GPR17 antibody. DAPI counterstained nuclei. Scale bars: 50 µm in A, C, F, H-K; 20 µm in B; 10 µm in D, E, G; 5 µm in B'.

Figure 3. Maturation pattern of postnatal GPR17 positive cells. A-D': changes in GPR17 and MBP expression from birth to adult stages. GPR17-positive cells were already present at birth (A). GPR17 expression increased over time (B,C) and declined in the adult cortex (D). MBP protein was instead not detectable until P7 (A',B'), whereas its expression level augmented at later time points (C',D'). E,F: graphs illustrate changes in GPR17- and GST-π-positive cell densities and anti-MBP staining intensity during postnatal development in GM (E) and WM (F). Only GPR17-/Olig2-positive cells were included in these quantifications. Densitometric quantifications of MBP labelling were normalized over P0 values: the increase in GPR17 positive cell number (P7 vs. P0, $P<0.05$) precedes GST-π/MBP rise. Its subsequent decrease (P24 vs. adult, $P<0.05$) parallels oligodendrocyte maturation. Asterisks indicate statistically

significant differences in GPR17+ cell densities compared to P0 values (One way Anova, $P<0.05$). G: quantitative analysis of the fractions of GPR17-expressing Olig2-positive/GST-π-negative cells at distinct postnatal ages. H,I: cells displaying GPR17 staining in the ramifications were very rare at birth but progressively increased amongst all receptor+ cells at postnatal ages ($P<0.001$, all postnatal ages vs. P0; Chi-square test). J: western blot analysis of GPR17 and MAG proteins revealed the presence of GPR17 before MAG production has started. Furthermore, GPR17 protein appeared downregulated before massive MAG protein production. The blot is representative of three independent experiments. P, postnatal day, GM, gray matter; WM, white matter; Gpi, GPR17 intracellular; Grm, GPR17 on cell membrane; KDa, kilodalton. Dotted lines, WM-GM border. Scale bars: 50 μm.

Figure 4. GPR17 expression in immature NG2-expressing cells during the fourth week of life. A-A': at P24, GPR17 was found in the large majority of NG2 expressing cells. Arrowheads indicate GPR17-/NG2-double positive cells. B: quantifications of fractions of double positive cells over the GPR17 expressing subsets. C,C': representative example of colocalisation between NG2 and PLP/DM20 in gray matter (confocal stack comprising only 3 optical sections 1μm thick). DAPI (blue) counterstains nuclei. Scale bars: 20 μm.

Figure 5. Proliferative activity of GPR17 expressing cells and GPR17 induction in adult newly generated NG2+ cells. A,B: proportions of BrdU+ cells amongst GPR17+ and NG2+ cells in gray and white matter. Asterisks highlight statistically significant differences between GPR17- and NG2-positive proliferative fractions ($P<0.05$). BrdU was administered for 1, 3, 7 days in the drinking water before animals were sacrificed. C-C''': cells with somatic localization of GPR17 can actively divide in the adult intact GM as shown by both anti-Ki67 (green fluorescence) and

anti-BrdU (white) staining. D,E: histograms represent the densities of cells positive for Ki67 or for BrdU incorporated after a double pulse, and the corresponding fractions of GPR17-double positive cells in gray (D) and white matter respectively (E). H,I: timing of GPR17 induction in fast proliferating cells labelled by a double BrdU pulse. GPR17 was detected in about half of the newborn cells but its expression declined over time. J,K: a similar pattern of receptor induction was found when monitoring GPR17 expression in a larger pool of both fast and slow proliferating cells tagged by a continuous BrdU administration for 2 weeks. F,G,L,M: micrographs illustrate GPR17+ cells retaining BrdU after 2 or 10 weeks. Asterisks indicate significant statistical differences in GPR17+/BrdU+ cell densities between distinct time points (One-way Anova; $P<0.05$). Arrowheads in (F,G,L,M) indicate GPR17-/BrdU- double positive cells. h, hours; d, days, wks, weeks. Scale bars: 10 µm in C, 50 µm in F,G,L,M .

Figure 6. GPR17 reactivity after cortical stab-wound. A-D: micrographs show anti-GPR17 labelling in the intact cortex (contralateral hemisphere, A) and in the stab-wounded tissue (B-D) at different days post lesion (dpl). Immediately after damage, GPR17+ cells decreased in number (B, 1dpl), but increased again at later time points (C, 7dpl). At 30 dpl the density of GPR17 positive cells appeared similar to that of the intact condition (D). E,H: post-injury changes of GPR17- or NG2- positive cell densities in gray (E) and white (H) matter territories. Asterisks indicate statistically significant differences (One way Anova, $P<0.05$) in post-lesion GPR17+ cell densities compared to intact values. F,I: cellular localization of GPR17 staining after lesion in gray (F) and white (I) matter. Asterisks in (F) indicate a significant difference in the percentage of cells with labelling in both somata and ramifications compared to the intact condition (Chi-square test; ** $P<0.01$; *** $P<0.001$). G,J: BrdU incorporation in GPR17- or NG2-positive cells after stab-wound, during 1 week of BrdU delivery in drinking water. Asterisk

in G highlights the difference (t-test, *P*<0.05) between the BrdU incorporating fractions of all GPR17+ and NG2+ cells (gray matter, 1dpl). CTRL, contralateral; SW, stab-wound; dpl, days post lesion, Gpi, GPR17 intracellular; Grm, GPR17 on cell membrane. Solid lines, lesion track; dotted lines, gray/white matter boundary. Scale bars: 50 μm.

Figure 7. GPR17 reactivity upon chronic amyloidosis. A,B: GPR17 expression in wild-type animals and age-matched APPPS1 mice. B': GPR17+ cells were found close to β-amyloid plaques (blue), where also reactive microglia (red) was detected. C: histograms depict the increase in GPR17+ and NG2+ cell densities in the gray matter (GM) of APPPS1 animals compared to wild type ones. Asterisks point to statistically significant differences (t-test, *P*<0.05). D: proportions of GPR17 positive cells with intracellular or diffuse (soma and processes) receptor localization in wild type and APPPS1 mice within 50 μm from plaques or in more distant gray matter parenchymal areas. At difference with the wild type parenchyma and with areas far from the plaque border, the vast majority of cells displayed high GPR17 in the processes (Grm) close to amyloid aggregates. Asterisks indicate the significant increase in the Grm fraction in the vicinity of plaques compared to wild type values (Chi test, *** *P*<0.001). E: BrdU incorporation in GM GPR17- or NG2-positive cells of wild type and APPPS1 mice after 1 week BrdU administration in the drinking water. While NG2 positive cells maintained a proliferative activity similar to that of wild type mice, BrdU incorporation almost doubled in GPR17 positive cells of APPPS1 animals. Asterisk highlights statistically significant difference (t-test, *P*<0.05). WT, wild type; Gpi, GPR17 intracellular; Grm, GPR17 on cell membrane. Scale bars: 50 μm.

	GPR17 expression pattern	
	Gpi ⟶	**Grm**
Precursor		
PDGFRa	+	-
NG2	+	+,+/-
Premyelinating		
PLP/DM20	-	+/-
CD9	-	+/-
Mature/Myelinating		
RIP	-	-
GST-π	-	-
PLP1	-	-
MAG	-	-
MBP	-	-

Table 1. GPR17 during oligodendrocyte differentiation. Red arrows indicate the progression from immature stages toward more advanced phenotypes**.**

Figure 1

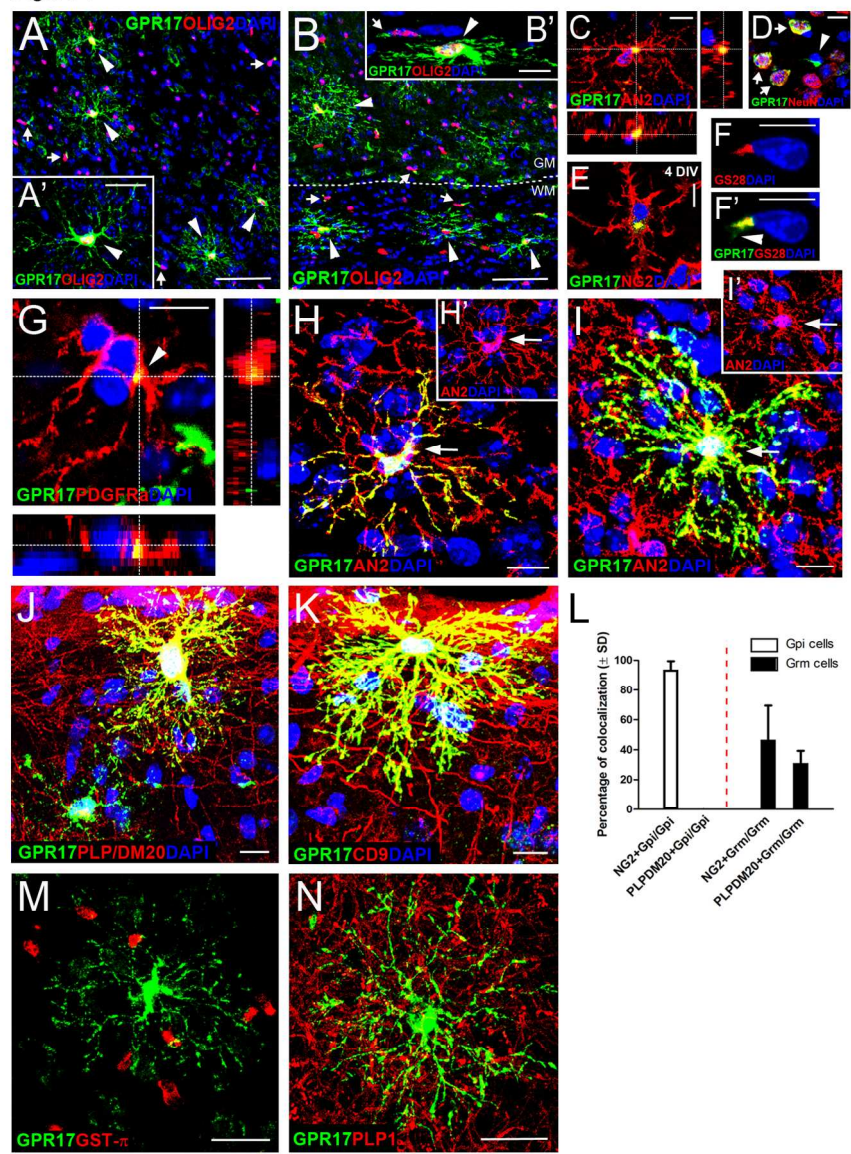
Figure 1. Phenotype of GPR17-expressing cells in the adult cortex. A-B': in the intact cortex, cells with either intracellular (Gpi type, arrows) or radiate (Grm type, arrowheads) GPR17 staining displayed Olig2 positivity in both gray (A,A') and white matter (B,B'). However, GPR17+/Olig2+ cells represented only a fraction of all Olig2+ cells (A,B). C,E, C-G: intracellular GPR17 spots belonged to NG2- (red in C, single confocal plane, and E, cell in vitro) and PDGFRa- (red in G, single confocal plane) expressing cells while diffuse somatic punctate staining corresponded to neurons (D). It often localized to the Golgi apparatus (red in F, immunostained with anti-GS28 antibody) or included also the starting segments of 1 or 2 cell processes (arrowhead in F'). H-I': NG2 positive Grm cells (labelled by anti-AN2 antibody) with distinct morphologies and receptor expression levels. J-K: Grm cells with intense receptor staining and broad radiating processes express premyelination markers. M,N: no colocalisation was found between GPR17 and markers for mature oligodendrocytes, such as GST-π (M) and PLP1 (N). Micrographs are confocal stacks comprising 15-20 optical sections 1mm thick. Somatic yellow pixels in J,K resulted from the overlapping of distinct optical images. L: quantifications of fractions of double positive cells over the GPR17 expressing subsets. DAPI

(blue) counterstains nuclei. The dotted line in (B) indicates the boundary between gray and white matter. GM, gray matter; WM, white matter; Gpi, intracellular GPR17 protein; Grm, GPR17 receptor on cell membrane. Scale bars: 50 µm in A, B; 10 µm in B'-K; 20 µm in A', M, N.
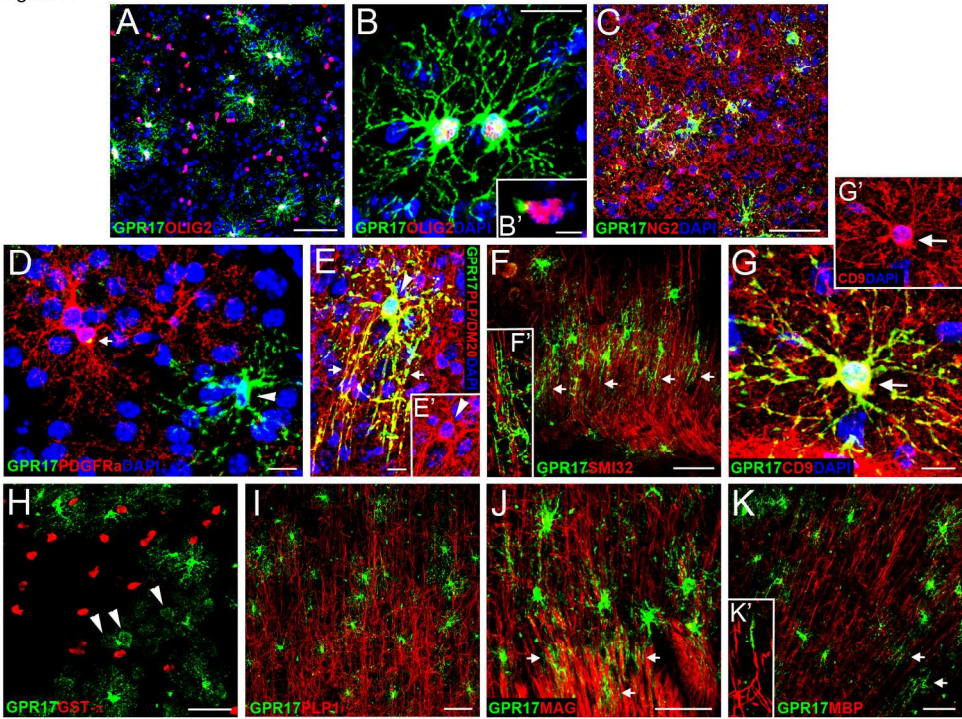
134x187mm (300 x 300 DPI)

Figure 2. Phenotype of GPR17-expressing cells during postnatal development. A-B': GPR17 is expressed in a subset of Olig2+ cells in the immature cerebral cortex. Both Grm (B) and Gpi (B') cell types were present among postnatal GPR17+ cells. C: virtually all GPR17+ cells coexpressed NG2. D: cells with intracellular GPR17 protein exhibited PDGFRa positivity. E, G: cells with high levels of receptor expression were stained also by anti PLP/DM20 (E, E') or CD9 (G, G') antibodies. H-K: no colocalisation was found with markers for mature oligodendrocytes, such as GST-π (H), PLP1 (I), MAG (J) and MBP (K). Some GPR17 processes run in parallel and intercalated with SMI32+ axons (F, F') and myelin tracts (J-K'). Micrographs are confocal stacks comprising 15-20 optical sections 1µm thick. Yellow pixels in H-J resulted from the overlapping of distinct optical images. No marker colocalisation was found in single optical sections. All micrographs are obtained from P14 cortex, with the exception of (C) obtained from a P7 brain. Arrowheads in (H) indicate neurons labelled by anti-GPR17 antibody. DAPI counterstained nuclei. Scale bars: 50 µm in A, C, F, H-K; 20 µm in B; 10 µm in D, E, G; 5 µm in B'.
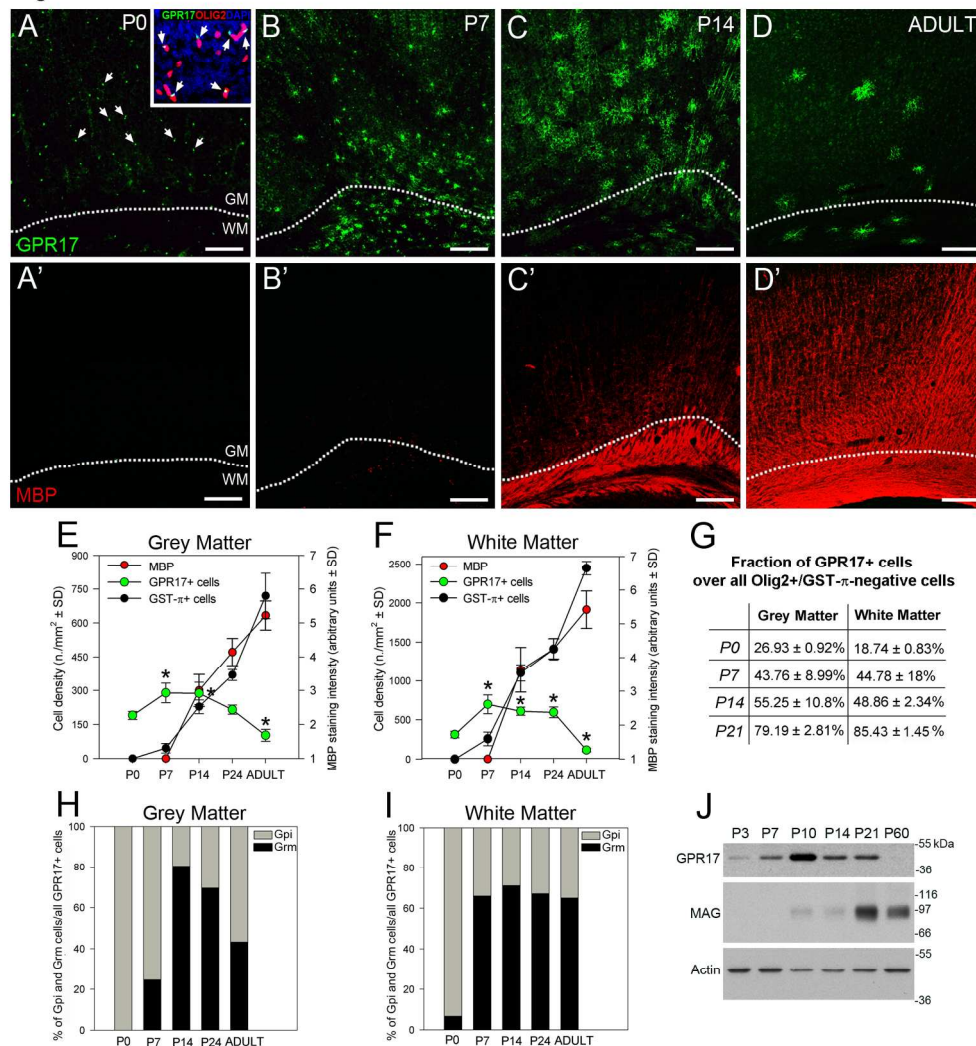180x137mm (300 x 300 DPI)

Figure 3

Figure 3. Maturation pattern of postnatal GPR17 positive cells. A-D': changes in GPR17 and MBP expression from birth to adult stages. GPR17-positive cells were already present at birth (A). GPR17 expression increased over time (B,C) and declined in the adult cortex (D). MBP protein was instead not detectable until P7 (A',B'), whereas its expression level augmented at later time points (C',D'). E,F: graphs illustrate changes in GPR17- and GST-п-positive cell densities and anti-MBP staining intensity during postnatal development in GM (E) and WM (F). Only GPR17-/Olig2-positive cells were included in these quantifications. Densitometric quantifications of MBP labelling were normalized over P0 values: the increase in GPR17 positive cell number (P7 vs P0, P<0.05) precedes GST-п/MBP rise. Its subsequent decrease (P24 vs adult, P<0.05) parallels oligodendrocyte maturation. Asterisks indicate statistically significant differences in GPR17+ cell densities compared to P0 values (One way Anova, P<0.05). G: quantitative analysis of the fractions of GPR17-expressing Olig2-positive/GST-п-negative cells at distinct postnatal ages. H,I: cells displaying GPR17 staining in the ramifications were very rare at birth but progressively increased amongst all receptor+ cells at postnatal ages (P<0.001, all postnatal ages vs P0; Chi-square test). J: western blot analysis of GPR17 and MAG proteins revealed the presence of GPR17 before MAG production has started. Furthermore, GPR17 protein appeared downregulated before massive MAG protein production. The blot is representative of three independent experiments. P, postnatal day, GM, gray matter; WM, white matter; Gpi, GPR17 intracellular; Grm, GPR17 on cell membrane; KDa, kilodalton. Dotted lines, WM-GM border. Scale bars: 50 µm.

180x199mm (300 x 300 DPI)

Figure 4

Figure 4. GPR17 expression in immature NG2-expressing cells during the fourth week of life. A-A': at P24, GPR17 was found in the large majority of NG2 expressing cells. Arrowheads indicate GPR17-/NG2-double positive cells. B: quantifications of fractions of double positive cells over the GPR17 expressing subsets. C,C': representative example of colocalisation between NG2 and PLP/DM20 in gray matter (confocal stack comprising only 3 optical sections 1μm thick). DAPI (blue) counterstains nuclei. Scale bars: 20 μm.
85x67mm (300 x 300 DPI)

Figure 5

Figure 5. Proliferative activity of GPR17 expressing cells and GPR17 induction in adult newly generated NG2+ cells. A,B: proportions of BrdU+ cells amongst GPR17+ and NG2+ cells in gray and white matter. Asterisks highlight statistically s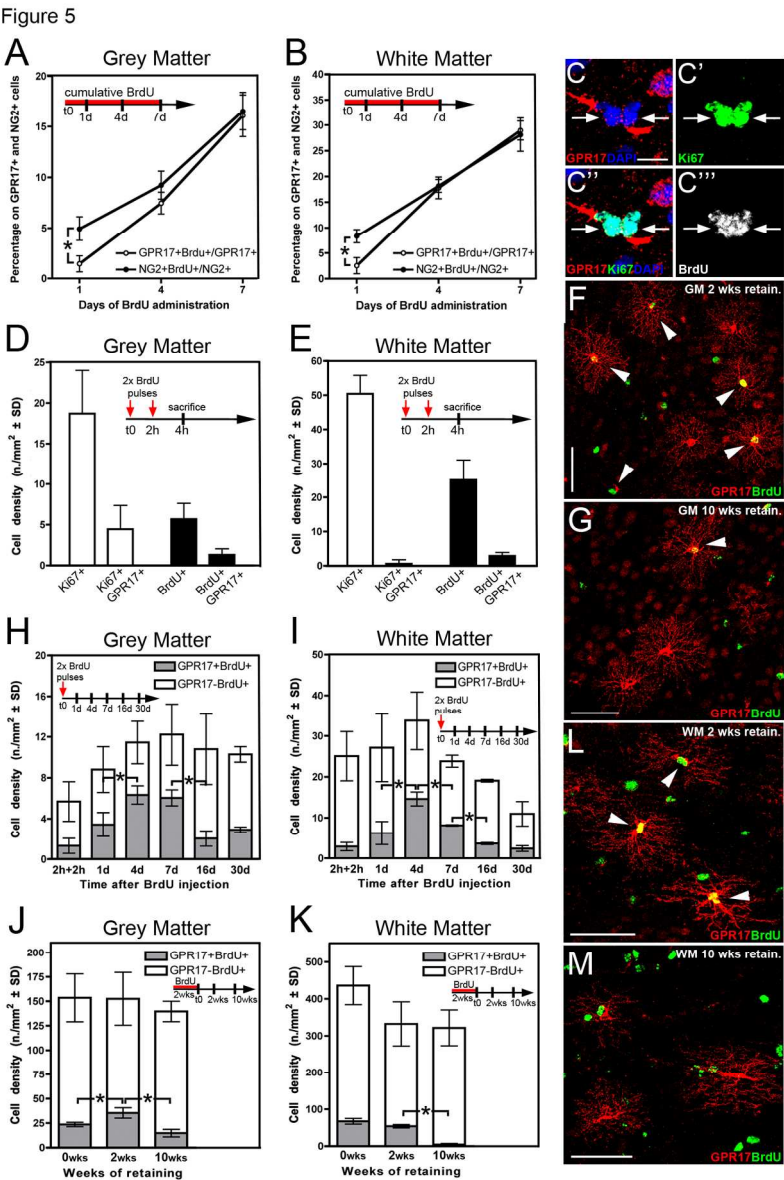ignificant differences between GPR17- and NG2-positive proliferative fractions (P<0.05). BrdU was administered for 1, 3, 7 days in the drinking water before animals were sacrificed. C-C''': cells with somatic localization of GPR17 can actively divide in the adult intact GM as shown by both anti-Ki67 (green fluorescence) and anti-BrdU (white) staining. D,E: histograms represent the densities of cells positive for Ki67 or for BrdU incorporated after a double pulse, and the corresponding fractions of GPR17-double positive cells in gray (D) and white matter respectively (E). H,I: timing of GPR17 induction in fast proliferating cells labelled by a double BrdU pulse. GPR17 was detected in about half of the newborn cells but its expression declined over time. J,K: a similar pattern of receptor induction was found when monitoring GPR17 expression in a larger pool of both fast and slow proliferating cells tagged by a continuous BrdU administration for 2 weeks. F,G,L,M: micrographs illustrate GPR17+ cells retaining BrdU after 2 or 10 weeks. Asterisks indicate significant statistical differences in GPR17+/BrdU+ cell densities

between distinct time points (One-way Anova; $P<0.05$). Arrowheads in (F,G,L,M) indicate GPR17-/BrdU- double positive cells. h, hours; d, days, wks, weeks. Scale bars: 10 µm in C, 50 µm in F,G,L,M .
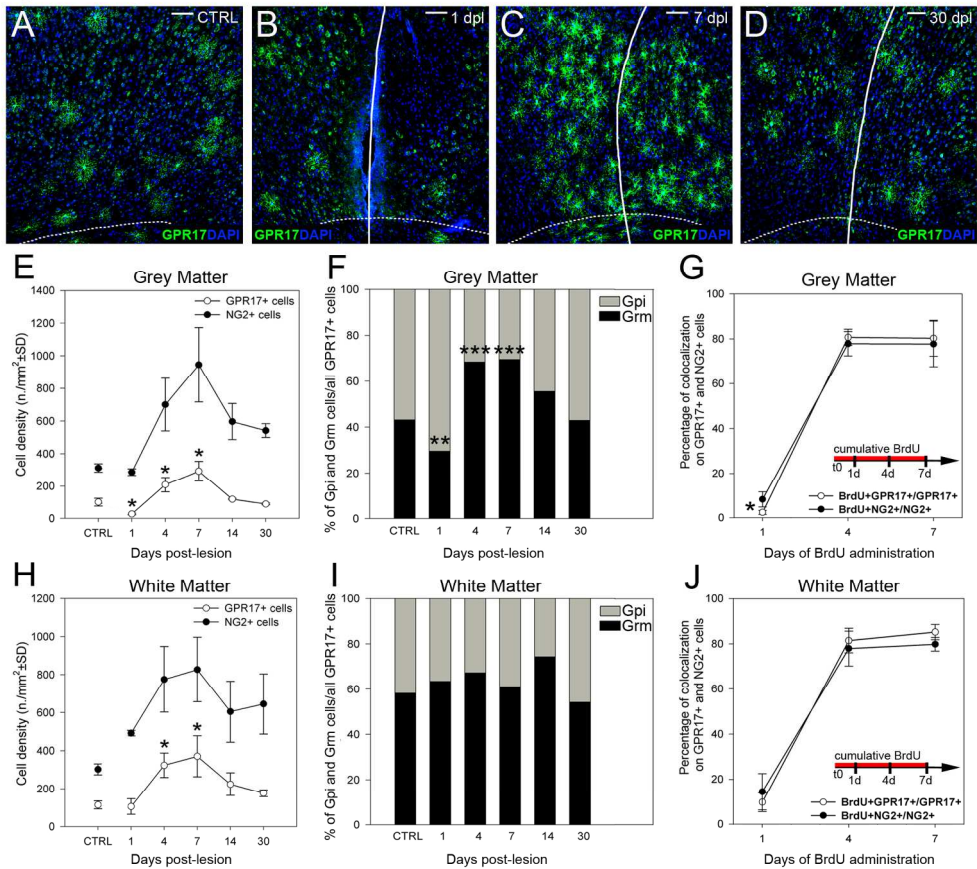141x207mm (300 x 300 DPI)

Figure 6. GPR17 reactivity after cortical stab-wound. A-D: micrographs show anti-GPR17 labelling in the intact cortex (contralateral hemisphere, A) and in the stab-wounded tissue (B-D) at different days post lesion (dpl). Immediately after damage, GPR17+ cells decreased in number (B, 1dpl), but increased again at later time points (C, 7dpl). At 30 dpl the density of GPR17 positive cells appeared similar to that of the intact condition (D). E,H: post-injury changes of GPR17- or NG2- positive cell densities in gray (E) and white (H) matter territories. Asterisks indicate statistically significant differences (One way Anova, $P<0.05$) in post-lesion GPR17+ cell densities compared to intact values. F,I: cellular localization of GPR17 staining after lesion in gray (F) and white (I) matter. Asterisks in (F) indicate a significant difference in the percentage of cells with labelling in both somata and ramifications compared to the intact condition (Chi-square test; ** $P<0.01$; *** $P<0.001$). G,J: BrdU incorporation in GPR17- or NG2-positive cells after stab-wound, during 1 week of BrdU delivery in drinking water. Asterisk in G highlights the difference (t-test, $P<0.05$) between the BrdU incorporating fractions of all GPR17+ and NG2+ cells (gray matter, 1dpl). CTRL, contralateral; SW, stab-wound; dpl, days post lesion, Gpi, GPR17 intracellular; Grm, GPR17 on cell membrane. Solid lines, lesion track; dotted lines, gray/white matter boundary. Scale bars: 50 μm.
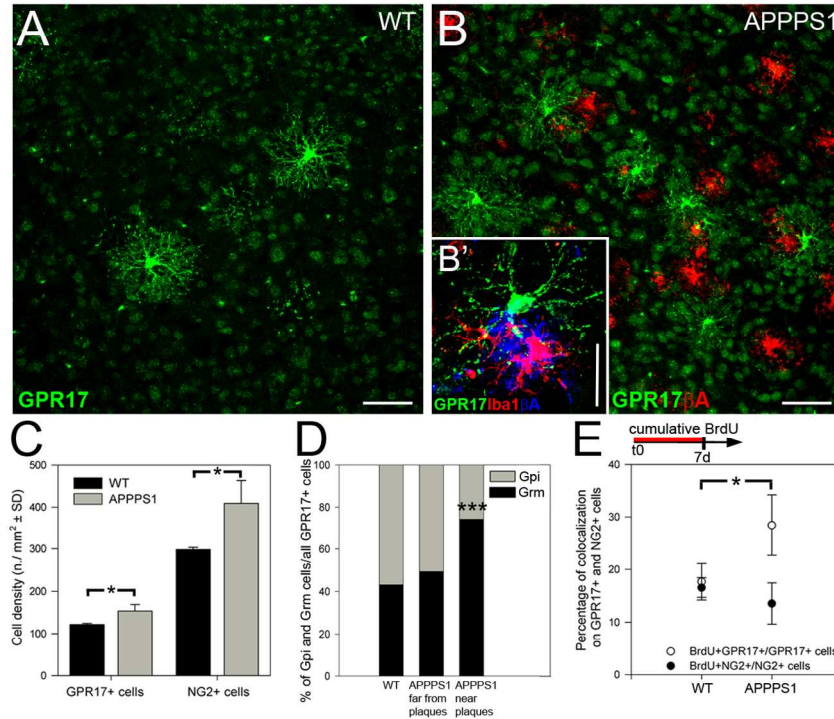180x167mm (300 x 300 DPI)

Figure 7

Figure 7. GPR17 reactivity upon chronic amyloidosis. A,B: GPR17 expression in wild-type animals and age-matched APPPS1 mice. B': GPR17+ cells were found close to β-amyloid plaques (blue), where also reactive microglia (red) was detected. C: histograms depict the increase in GPR17+ and NG2+ cell densities in the gray matter (GM) of APPPS1 animals compared to wild type ones. Asterisks point to statistically significant differences (t-test, P<0.05). D: proportions of GPR17 positive cells with intracellular or diffuse (soma and processes) receptor localization in wild type and APPPS1 mice within 50 μm from plaques or in more distant gray matter parenchymal areas. At difference with the wild type parenchyma and with areas far from the plaque border, the vast majority of cells displayed high GPR17 in the processes (Grm) close to amyloid aggregates. Asterisks indicate the significant increase in the Grm fraction in the vicinity of plaques compared to wild type values (Chi test, *** P<0.001). E: BrdU incorporation in GM GPR17- or NG2-positive cells of wild type and APPPS1 mice after 1 week BrdU administration in the drinking water. While NG2 positive cells maintained a proliferative activity similar to that of wild type mice, BrdU incorporation almost doubled in GPR17 positive cells of APPPS1 animals. Asterisk highlights statistically significant difference (t-test, P<0.05). WT, wild type; Gpi, GPR17 intracellular; Grm, GPR17 on cell membrane. Scale bars: 50 μm.
129x104mm (300 x 300 DPI)

Supporting information

Table 1. Primary antibodies used for immunohistology

Antibody	Targeted molecule	Host	Concentration	Source
Anti-AN2*	Mouse homologue of NG2 (Nerve/glial proteoglycan 2; expressed by postnatal and adult oligodendrocyte precursors)	Rat	1:100	Kind gift of Miltenyi (Biotech GmbH, Bergisch Gladbach,DE) and of J. Trotter (Johannes Gutenberg University of Mainz, DE)
Anti-βA (6E10 clone)	β-amyloid (extracellular plaques in APPPS1 mice)	Mouse	1:300	Covance, Princeton, NJ
Anti-BrdU	5-bromo-2'-deoxyuridine (DNA analog incorporated during the S-phase of the cell cycle)	Rat	1:500	ABcam, Cambridge, UK
Anti-CD9 (KMC8)	Tetraspanin protein CD9 (expressed by pre-myelinating oligodendrocytes)	Rat	1:25	BD transduction laboratories, Mississauga, ON
Anti-GFAP	Glial fibrillary acid protein (expressed by astrocytes)	Rabbit	1:1000	Dakopatts, Glostrup, Denmark
Anti–GPR17	G-protein coupled receptor 17	Rabbit	1:500 standard IF 1:10,000 TK IF	P. Rosa (CNR, Milan, Italy)
Anti–GPR17	G-protein coupled	Rabbit	1:250	Cayman

	receptor 17			Chemical, Ann Arbor, USA
Anti-GS28	Golgi SNARE of 28 kDa (integral membrane protein on the surface of the Golgi apparatus)	Mouse	1:50	StressGen Biotechnologies, Victoria, BC, Canada
Anti-GSTπ	Glutathione S-transferase-π (expressed by mature oligodendrocytes)	Rabbit	1:500	BD
Anti-Iba1	Ionized calcium-binding adaptor molecule 1 (expressed by microglia/macrophages)	Rabbit	1:1000	Wako Chemicals, Richmond,VA
Anti-Ki67	Nuclear protein (expressed in actively dividing cells)	Rabbit	1:1000	Thermo-Fisher, Rockford, IL
Anti-MAG	Myelin associated protein (expressed by myelinating oligodendrocytes)	Mouse	1:500	Chemicon
Anti-MBP	Myelin basic protein (expressed by myelinating oligodendrocytes)	Mouse	1:2000	Covance
Anti- NG2*	Nerve/glial proteoglycan 2 (expressed by postnatal and adult oligodendrocyte precursors)	Rabbit	1:200	Chemicon

Anti- Olig2	Olig2 transcription factor (expressed in the oligodendroglial lineage)	Rabbit	1:500	Chemicon
Anti-Oligodendrocytes (RIP)	2',3'-cyclic nucleotide 3'-phosphodiesterase (expressed by mature oligodendrocytes)	Mouse	1:500	Chemicon
Anti-PDGFRa (APA-5 clone)	Platelet-derived growth factor receptor alpha (expressed by oligodendrocyte precursors)	Rat	1:100	BD
Anti-PLP	Proteolipid protein (the first myelin protein)	Mouse	1:100	Chemicon
Anti-PLP/DM20 (AA3 clone)	Recognises both the immature and mature spliced products of the Proteolipid Protein (PLP) gene (the immature one is expressed by pre-myelinating oligodendrocytes)	Rat	1:5	Kind gift of B. Zalc (INSERM, Salpetriere Hospital, Paris)
Anti-S100b	Calcium binding protein (expressed by astrocytes)	Mouse	1:1000	Sigma
Anti-SMI32	Neurofilament protein H (expressed by neurons)	Mouse	1:500	Sternberger, Baltimore, MD
Anti-vimentin	Astroglial cells	Mouse	1:20	Hybridoma Bank

IF, immunofluorescence; TK, tyramide kit; *on pictures, AN2 or NG2 indicate stainings obtained with the rat or rabbit antibody, respectively, while in the text we refer to the antigen as NG2.

Table 2. Secondary antibodies used in this study

Antibody	Host species	Concentration	Source
Anti-mouse Cy3	donkey	1:500	Jackson ImmunoResearch Laboratories, West Grove, PA
Anti-mouse AMCA	horse	1:200	Vector Laboratories, Burlingame, CA
Anti-mouse FITC	horse	1:200	Vector Laboratories
Anti-mouse IgM-Alexa 546	donkey	1:500	Molecular Probes Inc, Eugene Oregon
Anti-rabbit AlexaFluor546	goat	1:500	Molecular Probes
Anti-rabbit FITC	Goat	1:200	Vector Laboratories
Anti-rat FITC	rabbit	1:200	Vector Laboratories
Anti-rat Cy3	donkey	1:500	Jackson ImmunoResearch Laboratories

SUPPORTING INFORMATION FIGURE LEGENDS

Supporting Information Figure 1. BrdU administration protocols and cortical areas analysed in this study. A: schematic representation of the protocols applied to deliver the DNA-base analogue BrdU to mice. B: the drawing depicts a coronal section representative of those inspected for quantifications. A grey matter area of about 500 μm^2 in the sensorimotor cortex was analyzed together with the corresponding subcortical white matter tract in the intact, wild type and APPPS1 cortices and upon stab-wound (gray areas). BrdU, 5-bromo-2-deoxyuridine; d, day; h, hours; wks, weeks; P, postnatal day; CTRL, contralateral, WT, wild type; SW, stab-wound.

Supporting Information Figure 2. Frequency distribution of Grm soma diameters at adult ages and postnatal day 24. Average diameters were measured for PDGFRa expressing cells, PLP/DM20+ premyelinating oligodendrocytes and Grm cells at mature stages (A) and postnatal times (C) in the cortical white matter. B,D: frequencies of GPR17+ cell values were plotted and colour-coded according to their correspondence to diameters typical of PDGFRa+ or PLP/DM20+ cells. Bin width, 1 μm.

Supporting Information Figure 3. Spatio-temporal pattern of Grm cell maturation in cortical gray and white matter during postnatal development. A,B: graphs illustrate the frequency distribution of Grm cells at defined distances from the midline in the white matter (A) or at defined distances from the gray-white matter border (B). Grm cells were located in the lateral white matter at P0 (black line) and reached an homogenous distribution throughout the whole latero-medial white matter extension at subsequent time points (red and green lines). No Grm cells were found in the gray matter at P0 (black line), but later on matured according to a

ventral-to-dorsal gradient (red and green lines). P, postnatal day; Grm, GPR17 on cell membrane.
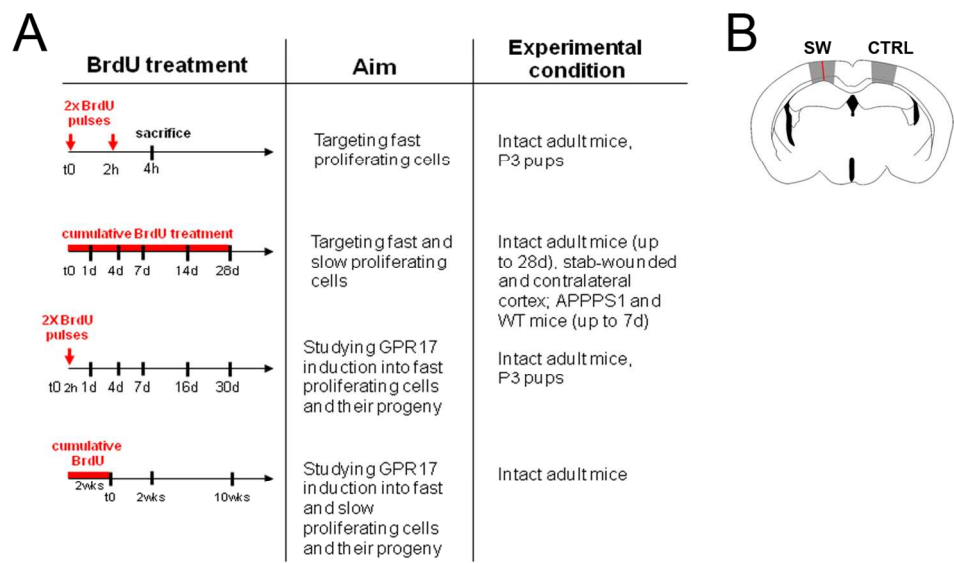
Supporting Information Figure 4. GPR17 induction in newly-generated oligodendrocyte precursors at postnatal stage. After a double BrdU pulse in P3 mice, in the postnatal gray matter GPR17 was transiently induced only in a fraction of all newborn Olig2+ cells (34.76 ± 6.00% at the 7d peak). Increase in cortical volume as well as BrdU dilution during cell divisions may contribute to the decrease of Olig2+/BrdU+ cell density at 30d. Asterisks indicate statistical significant differences in GPR17+/BrdU+ cell densities at distinct time points (One-way Anova; $P<0.05$). d, day; h, hours; P, postnatal.

Supporting Information Figure 5. GPR17 mRNA quantification after acute and chronic cortical injury The expression level of GPR17 transcript was evaluated by means of quantitative Real Time RT-PCR in the cerebral cortex of stab-wounded (A, SW) and APPPS1 mice (B). Total RNA was extracted from pieces of cerebral tissue corresponding to those illustrated in Suppl. Fig. 1B. As for measurements on histological sections, the contralateral intact side was considered as control for stab-wounded cortex. A: at 1 day after SW, the level of GPR17 mRNA transiently decrease compared to the contralateral value. This decrease was followed by an upregulation that lasted up to 7 days after lesion and subsequently declined. B: despite a moderate increase, GPR17 mRNA in APPPS1 cortex did not significantly differ from that of aged-matched WT mice. Asterisks in A indicate statistical differences between SW and CTRL at each time point (Two-ways Anova $P<0.05$). CTRL, contralateral, SW stab-wound, WT, wild type.

Supporting Information Figure 6. Spatio-temporal pattern of Gpi and Grm cell reactivity in the cortical GM after stab-wound. After acute lesion, Gpi and Grm GPR17+ cells displayed distinct spatio-temporal distributions. Graphs in A, B and C illustrate the frequency distribution of Gpi (black lines) and Grm (red lines) cells at defined distances from the stab-wound track (SW). Black (Gpi) and red (Grm) circles in (A) indicate the frequency values in the intact tissue. Immediately after lesion (1dpl, A), Grm cells completely disappeared in the proximity of the SW site and displayed an early reactivity distally to the injury track. Gpi cells remained homogenously distributed in the cortical parenchyma. B: at 4 dpl Gpi cells were increased in density at the injury site whereas Grm cells remained mostly located far away from the lesion. Grm cells appeared close to SW at 7 dpl, where both Gpi and Grm densities were higher compared to contralateral values (C). dpl day post-lesion; Gpi, GPR17 intracellular; Grm, GPR17 on cell membrane; CTRL contralateral; SW, stab-wound.

Supporting Information Figure 7. Accumulation of GPR17+ cells at sites of myelin disruption A-A'': in the intact white matter, GPR17 expressing cells were dispersed amongst MBP-positive fibres. B,B': stereotaxic injection into the subcortical white matter of lysolecithin (1% lysolecithin in 0.9% NaCl) induced a focal disruption of MBP-labeled compact myelin (compare panels B,B' in lesioned animals with panels A, A'). B'': ten days after toxin injections, at times when spontaneous myelin repair starts (Woodruff and Franklin, 1999; Birgbauer et al., 2004) clusters of GPR17-positive cells appeared in the area of damaged myelin. These cells coexpressed the transcription factor Olig2 (red fluorescence, C). Scale bars: 50 μm.

Supp. Info. Figure 1

Supporting Information Figure 1. BrdU administration protocols and cortical areas analysed in this study. A: schematic representation of the protocols applied to deliver the DNA-base analogue BrdU to mice. B: the drawing depicts a coronal section representative of those inspected for quantifications. A grey matter area of about 500 µm2 in the sensorimotor cortex was analyzed together with the corresponding subcortical white matter tract in the intact, wild type and APPPS1 cortices and upon stab-wound (gray areas). BrdU, 5-bromo-2-deoxyuridine; d, day; h, hours; wks, weeks; P, postnatal day; CTRL, contralateral, WT, wild type; SW, stab-wound.
123x78mm (300 x 300 DPI)

Supp. Info. Figure 2
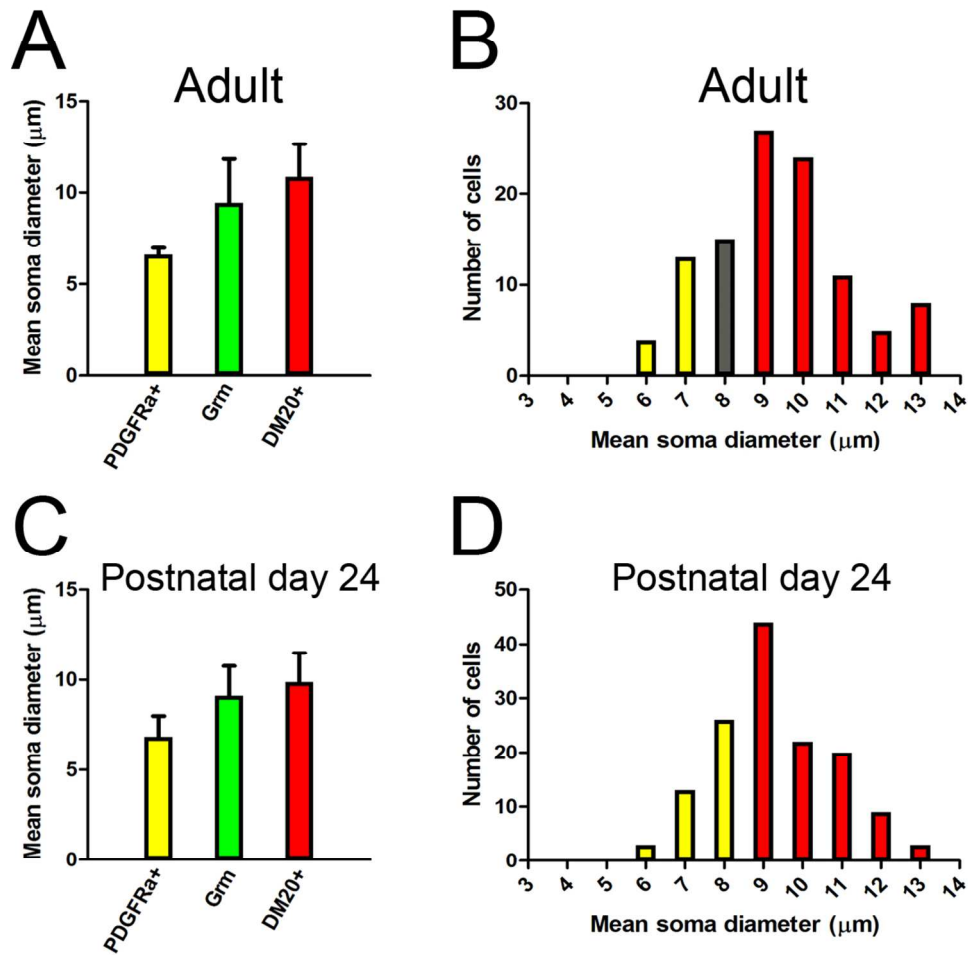
Supporting Information Figure 2. Frequency distribution of Grm soma diameters at adult ages and postnatal day 24. Average diameters were measured for PDGFRa expressing cells, PLP/DM20+ premyelinating oligodendrocytes and Grm cells at mature stages (A) and postnatal times (C) in the cortical white matter. B,D: frequencies of GPR17+ cell values were plotted and colour-coded according to their correspondence to diameters typical of PDGFRa+ or PLP/DM20+ cells. Bin width, 1 μm.
103x105mm (300 x 300 DPI)

Supp. Info. Figure 3

Supporting Information Figure 3. Spatio-temporal pattern of Grm cell maturation in cortical gray and white matter during postnatal development. A,B: graphs illustrate the frequency distribution of Grm cells at defined distances from the midline in the white matter (A) or at defined distances from the gray-white matter border (B). Grm cells were located in the lateral white matter at P0 (black line) and reached an homogenous distribution throughout the whole latero-medial white matter extension at subsequent time points (red and green lines). No Grm cells were found in the gray matter at P0 (black line), but later on matured according to a ventral-to-dorsal gradient (red and green lines). P, postnatal day; Grm, GPR17 on cell membrane.
180x105mm (300 x 300 DPI)

Supp. Info. Figure 4
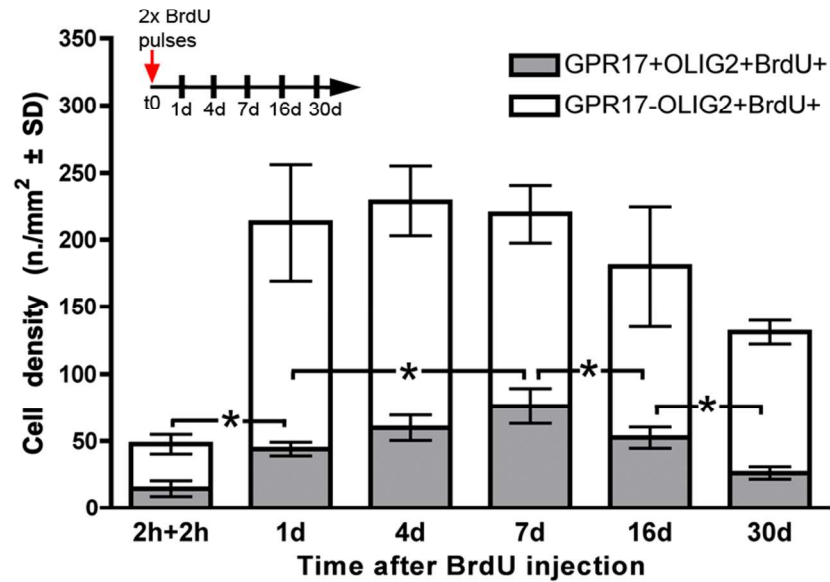
Supporting Information Figure 4. GPR17 induction in newly-generated oligodendrocyte precursors at postnatal stage. After a double BrdU pulse in P3 mice, in the postnatal gray matter GPR17 was transiently induced only in a fraction of all newborn Olig2+ cells (34.76 ± 6.00% at the 7d peak). Increase in cortical volume as well as BrdU dilution during cell divisions may contribute to the decrease of Olig2+/BrdU+ cell density at 30d. Asterisks indicate statistical significant differences in GPR17+/BrdU+ cell densities at distinct time points (One-way Anova; P<0.05). d, day; h, hours; P, postnatal.
87x61mm (300 x 300 DPI)

Supp. Info. Figure 5

Supporting Information Figure 5. GPR17 mRNA quantification after acute and chronic cortical injury The expression level of GPR17 transcript was evaluated by means of quantitative Real Time RT-PCR in the cerebral cortex of stab-wounded (A, SW) and APPPS1 mice (B). Total RNA was extracted from pieces of cerebral tissue corresponding to those illustrated in Suppl. Fig. 1B. As for measurements on histological sections, the contralateral intact side was considered as control for stab-wounded cortex. A: at 1 day after SW, the level of GPR17 mRNA transiently decrease compared to the contralateral value. This decrease was followed by an upregulation that lasted up to 7 days after lesion and subsequently declined. B: despite a moderate increase, GPR17 mRNA in APPPS1 cortex did not significantly differ from that of aged-matched WT mice. Asterisks in A indicate statistical differences between SW and CTRL at each time point (Two-ways Anova P<0.05). CTRL, contralateral, SW stab-wound, WT, wild type.
180x93mm (300 x 300 DPI)

Supp. Info. Figure 6

Supporting Information Figure 6. Spatio-temporal pattern of Gpi and Grm cell reactivity in the cortical GM after stab-wound. After acute lesion, Gpi and Grm GPR17+ cells displayed distinct spatio-temporal distributions. Graphs in A, B and C illustrate the frequency distribution of Gpi (black lines) and Grm (red lines) cells at defined distances from the stab-wound track (SW). Black (Gpi) and red (Grm) circles in (A) indicate the frequency values in the intact tissue. Immediately after lesion (1dpl, A), Grm cells completely disappeared in the proximity of the SW site and displayed an early reactivity distally to the injury track. Gpi cells remained homogenously distributed in the cortical parenchyma. B: at 4 dpl Gpi cells were increased in density at the injury site whereas Grm cells remained mostly located far away from the lesion. Grm cells appeared close to SW at 7 dpl, where both Gpi and Grm densities were higher compared to contralateral values (C). dpl day post-lesion; Gpi, GPR17 intracellular; Grm, GPR17 on cell membrane; CTRL contralateral; SW, stab-wound.
180x81mm (300 x 300 DPI)

Supp. Info. Figure 7

Supporting Information Figure 7. Accumulation of GPR17+ cells at sites of myelin disruption A-A″: in the intact white matter, GPR17 expressing cells were dispersed amongst MBP-positive fibres. B,B′: stereotaxic injection into the subcortical white matter of lysolecithin (1% lysolecithin in 0.9% NaCl) induced a focal disruption of MBP-labeled compact myelin (compare panels B,B′ in lesioned animals with panels A, A′). B″: ten days after toxin injections, at times when spontaneous myelin repair starts (Woodruff and Franklin, 1999; Birgbauer et al., 2004) clusters of GPR17-positive cells appeared in the area of damaged myelin. These cells coexpressed the transcription factor Olig2 (red fluorescence, C). Scale bars: 50 µm.
129x70mm (300 x 300 DPI)

The GPR17 receptor in NG2 expressing cells: focus on in vivo cell maturation and participation in acute trauma and chronic damage

Enrica Boda[1, 2]*, Francesca Viganò[3,4]*, Patrizia Rosa[5], Marta Fumagalli[3], Vivien Labat-gest[1, 2], Filippo Tempia[1, 2, 6], Maria P. Abbracchio[3], Leda Dimou[4] and Annalisa Buffo[1, 2, 7]

[1]Department of Neuroscience, University of Turin, Turin, Italy

[2]Neuroscience Institute Cavalieri-Ottolenghi (NICO), Regione Gonzole 10 10043 Orbassano Turin, Italy

[3]Laboratory of Molecular and Cellular Pharmacology of Purinergic Transmission, Department of Pharmacological Sciences, University of Milan, Italy

[4]Institute of Physiology, Physiological Genomics, Ludwig-Maximilians-University, Pettenkoferstr. 12, 80336 Munich, Germany

[5]CNR Institute of Neuroscience, Department of Medical Pharmacology, Via Vanvitelli 32, Milan, Italy

[6]National Institute of Neuroscience-Italy (INN), Turin, Italy

[7]Neuroscience Institute of Turin (NIT), Turin, Italy

* These authors contributed equally to the work

Running title: GPR17 in NG2 expressing cells

Number of words in abstract, 25049; introduction, 54206; materials and methods: 1642; results, 356152; discussion, 1226; figure legends, 146452; references, 179711.

Total word number, 10482804

Figures, 7

Tables, 1

Supporting Information, 7 figures and legends, 2 tables

Author for correspondence:

Annalisa Buffo

Department of Neuroscience, University of Turin, Neuroscience Institute Cavalieri-Ottolenghi,

Neuroscience Institute of Turin

Regione Gonzole 10 10043 Orbassano Turin – Italy

Tel 00 39 011 6706614

Fax 00 39 011 6705449

Email: annalisa.buffo@unito.it

Abbreviations: +, positive; BrdU, 5-bromo-2-deoxyuridine; CNS, central nervous system; CTRL, contralateral; DAPI, 4',6-diamidino-2-phenylindole; d, days;dpi, days post injection; dpl, days post lesion; dpt, days post BrdU treatment; GM, gray matter; Grm, GPR17 receptor on cell membrane; GPR17, G-protein coupled receptor 17; Gpi, GPR17 protein intracellular; GST-π, glutathione S-transferase-π; h, hours; MAG, myelin associated glycoprotein; MBP, myelin basic protein; P, postnatal day; PLP1, proteolipid protein 1; RIP, 2',3'-cyclic nucleotide 3'-phosphodiesterase; RT, reverse-transcription; SW, stab-wound; wks, weeks; WM, white matter; WT, wild type.

Abstract

NG2-expressing cells comprise a population of cycling precursors that can exit the cell cycle and differentiate into mature oligodendrocytes. As a whole, they display heterogeneous properties and behaviours that remain unresolved at the molecular level, although partly interpretable as distinct maturation stages. To address this issue, we analyzed the expression of the GPR17 receptor, recently shown to decorate NG2-expressing cells and to operate as an early sensor of brain damage, in immature and adult oligodendrocyte progenitors in the intact brain and after injury. In both the early postnatal and adult cerebral cortex, distinct GPR17 protein localisations and expression levels define different stages of oligodendroglial maturation, ranging from the precursor phase to the premyelinating phenotype. As soon as cells exit mitosis, a fraction of NG2-expressing cells displays accumulation of GPR17 protein in the Golgi apparatus. GPR17 expression is subsequently upregulated and distributed to processes of cells that stop dividing, progressively lose NG2 positivity and assume pre-myelinating features. Absence of colabelling with mature markers or myelin proteins indicates that GPR17 is downregulated when cells complete their final maturation. BrdU-based fate-mapping demonstrated that a significant fraction of newly generated oligodendrocyte progenitors transiently upregulates GPR17 during their maturation. Importantly, we also found that GPR17 does not participate to the early reaction of NG2-expressing cells to damage, while it ~~s induction takes part in the nervous tissue reaction to damage~~ is induced at post-acute stages after injury. These findings identify GPR17 as a marker for progenitor progression within the oligodendroglial lineage and highlight GPR17 participation in post-acute reactivity of NG2 positive cells in different injury paradigms. ~~strengthen the possibility that receptor-expressing cells can be engaged to potentiate reparative responses to injury by specific pharmacological manipulations.~~

4

Introduction

Cells expressing the chrondroitin sulphate proteoglycan NG2 and displaying traits of the oligodendroglial lineage comprise an abundant population in the immature and adult central nervous system (CNS) (Butt et al., 2002; Nishiyama et al., 2002). These cells behave as precursors for mature oligodendrocytes *in vitro* and *in vivo*, and potentially for astrocytes and neurons (Nishiyama 2009; Boda and Buffo, 2010; Trotter et al., 2010). Furthermore, they represent the major population of cycling cells in the adult nervous tissue (Horner et al., 2000; Dawson et al., 2003; Simon et al., 2011), and respond to injury by increased proliferation (Butt et al., 2002; Simon et al., 2011). Notably, their multiple functions also encompass a tight interplay with neurons by synaptic signalling, expression of neurotransmitter receptors and generation of action potentials (Bakiri et al., 2009).

However, it is increasingly clear that NG2 positive (+) cells possess heterogeneous properties and behaviours, as indicated by myelination abilities in the adult gray and white matter (Dimou et al., 2008; Rivers et al., 2008), proliferative activity (reviewed in Nishiyama et al., 2009), response to neuronal activity (De Biase et al., 2010) and reaction to injury (Hampton et al., 2004; Lytle et al., 2009). Such diversity can be partly explained by distinct maturation stages (De Biase et al., 2010), but molecular markers are lacking to unambiguously resolve this point.

With the aim to gain insights into NG2+ cell heterogeneity, we focused on the G-protein coupled GPR17 receptor, which has been recently shown to be expressed by oligodendrocyte precursor cells (Lecca et al., 2008) and recognized as an interesting functional oligodendroglial modulator (Lecca et al., 2008; Chen et al., 2009; Fumagalli et al., 2011). GPR17 is activated by uracil nucleotides and cysteinyl leukotrienes (Ciana et al., 2006; Lecca et al., 2008; Pugliese et al., 2009). While uracil nucleotides and their sugar conjugates are gaining importance as

signalling mediators in the healthy CNS (Lecca and Ceruti, 2008), both classes of GPR17 endogenous agonists are massively released at the site of injury in traumatic, vascular and inflammatory pathologies (Ciceri et al., 2001; Melani et al., 2005; Buffo et al., 2010), where they activate tissue reactivity. GPR17 was shown to operate as a "sensor molecule" for these damage signals, orchestrating the early CNS reaction to stroke and spinal cord injury (Ciana et al., 2006; Lecca et al., 2008; Ceruti et al., 2009). These studies, however, did not examine whether GPR17 was specifically implicated in activating the response of NG2+ cells to injury. ~~While some aspects of GPR17 functions have been already unveiled, at present it is not clear~~ Further, it has remained so far undefined at which exact phase of oligodendroglial maturation the receptor is acting *in vivo*, and how GPR17 expressing cells behave during postnatal ontogenesis ~~and after injury~~.

~~In this study,~~To address these issues, we i) analysed the expression pattern and the proliferative behaviour of GPR17+ oligodendroglial cells in the postnatal and adult mouse cerebral cortex in the intact brain; ii) extended this analysis to models of traumatic brain injury and cerebral amiloidosis so to gain insights into the participation of GPR17 in the reaction of NG2+ cells to acute and chronic damage. We found that GPR17 transiently labels relevant fractions of NG2+ cells that upregulate the receptor after cell division and progress to the premyelinating stage. Furthermore, we show that GPR17 induction participates in the post-acute response to damage of oligodendroglial cells.

MATERIALS AND METHODS

Animals and surgical procedures

All experiments were performed on C57BL/6 mice (early postnatal and adult). Surgical procedures and perfusions were carried out under deep general anaesthesia (ketamine, 100 mg/kg; Ketavet, Bayern, Leverkusen, Germany; xylazine, 5 mg/kg; Rompun; Bayer, Milan, Italy). The experimental plan was designed according to the guidelines of the NIH, the European Communities Council (86/609/EEC), the state of Bavaria (under licence number 55.2-1-54-2531-144/07), the Italian law for care and use of experimental animals (DL116/92). It was also approved by the Italian Ministry of Health and the Bioethical Committee of the University of Turin.

Two-to-four month old mice underwent a stab-wound in the right cerebral cortex (Bregma from -0.4 mm to -2 mm, latero-lateral 1.5–2.5 mm) encompassing both gray and white matter and were sacrificed at different time-points after lesion (see results). As a model of chronic amyloid deposition, we examined 12 month-old C57BL/6-TgN (Thy1-APP$_{KM670/671NL}$; Thy1-PS1$_{L166P}$) mice (APPPS1) and wild-type littermates (Radde et al, 2006).

Proliferation, fate analysis and immunohistochemistry

To examine cell proliferation in intact, stab-wounded and APPPS1 mice we employed the thymidine analogue 5-bromo-2-deoxyuridine (BrdU, Sigma Aldrich, Milan, Italy), that is incorporated in the DNA during the S-phase of the cell cycle and remains into the DNA even when the cell exits the active phase of the cells cycle, therefore being suitable to detect not only active mitosis but also cells that had proliferated at the moment of BrdU administration (see Supp. Info. Fig. 1A; Buffo et al., 2005; Taupin, 2007; Dimou et al., 2008). Active proliferation (fast-proliferating cells) at the moment of analysis was revealed by either two

subsequent BrdU injections (100 mg/kg body weight for adult mice or 50 mg/kg body weight for pups, i.p.) performed at a 2 hour distance followed by sacrifice 2 hours after the last pulse, or by expression of Ki67 (an antigen present from S to M phases of the cell cycle, Taupin, 2007). To tag all cells that had proliferated within a defined time-window (including fast- and slow-proliferating cells as well as their post-mitotic progeny), BrdU (1mg/ml) was administered in drinking water until sacrifice. In case of stab-wound injury, BrdU treatment was initiated immediately after lesion. The kinetics of GPR17 expression in newly generated cells were evaluated by BrdU retaining after a double BrdU pulse (see above, 3 day old pups and adult mice) or after BrdU administration for 2 weeks (adult mice). BrdU incorporation into GPR17+ cells was assessed immediately after treatment and at different survival times (Supp. Info. Fig. 1A).

For histological analysis, animals were anaesthetized (as above) and transcardially perfused with 4% paraformaldehyde in phosphate buffer. Brains were postfixed, cryoprotected, and processed according to standard protocols (Buffo et al., 2005; Dimou et al., 2008). Adult brains were cut in 30 μm thick coronal sections collected in PBS. Brain slices of mice up to 14 days after birth (P14) were placed directly onto glass slides. The sections were stained to detect the expression of different antigens (see Supp. Info. Table1). Incubation with primary antibodies was made overnight at 4°C in PBS with 1.5% goat normal serum and 0.5% Triton-X 100. The sections were then exposed for two hours at room temperature to secondary antibodies (Supp. Info. Table 2). 4',6-diamidino-2-phenylindole (DAPI, Fluka, Milan, Italy) was used to visualize cell nuclei. Some sections were stained with the ApopTag fluorescein in situ apoptosis detection kit (Chemicon) to detect apoptotic cells. After processing, sections were mounted on microscope slides with Tris-glycerol supplemented with 10% Mowiol (Calbiochem, LaJolla, CA) or Aquapolymount (Hiss).

GPR17 was detected by means of affinity-purified antibodies (Supp. Info. Table 1; Ciana et al., 2006). Specificity of the "in house-made" antibody was tested by western blot analysis of total homogenates from Oli-neu cells, a mouse oligodendroglial cell line (Jung et al., 1995), transfected with a siRNA against the GPR17 gene (E. Parmigiani et al., unpublished). To reveal GPR17 expression either standard immunofluorescence procedures were applied (see above) or, for costaining of primary antibodies developed in the same species, the high sensitivity tyramide signal amplification kit (Perkin Elmer, Monza, Italy) was utilized according to the manufacturer's instruction (see also Buffo et al., 2005). NG2 expression was evaluated and confirmed with both rabbit and rat (AN2 clone) antibodies (Supp. Info. Table 1) that yielded comparable results. Stainings for CD9 and PLP/DM20 were performed as in Kukley et al. (2010). For PDGFRa labelling, post-fixation after perfusion was omitted. To facilitate BrdU recognition, slices were either treated with 2N HCl for 20 minutes at 37°C, followed by 10 minutes in borate buffer, or boiled for 20 minutes in citrate buffer before adding primary antibodies. This latter procedure was also applied for anti-Ki67 staining.

Primary oligodendrocyte precursor cultures

Primary cultures of oligodendrocyte precursors belonged to a previous set of experiments (Fumagalli et al., 2011). Coverslips stained with the anti-GPR17 antibody and mouse anti-NG2 antibody (1:200, Abcam, Cambridge, UK) were re-evaluated to assess the presence of the GPR17 protein in oligodendrocyte precursor somata.

Real time RT-PCR

Quantitative Real Time RT-PCR experiments were performed as in Boda et al., 2009. Briefly, mice (4-6 individuals per time point and experimental condition) were sacrificed (see above),

brains quickly removed under semi-sterile conditions and placed in ice-cold standard Ringer solution bubbled with 95% O_2- 5% CO_2. Thereafter, 400 μm thick coronal sections were prepared using a vibratome (Leica Microsystems GmbH, Wetzlar, Germany) and small pieces of intact or stab-wounded neocortex including the underlying white matter (WM) were dissected out and immediately frozen in -80°C 2-methylbutane before total RNA isolation (RNeasy micro kit, Qiagen, Milan, Italy). One μg of total RNA was reverse-transcribed (RT) to single stranded cDNA (High-Capacity cDNA Archive Kit, Applied Biosystems, Monza, Italy).

An ABI Prism 7000 Sequence Detection System (Applied Biosystems) was employed in combination with Taqman reagent-based chemistry (Applied Biosystems). Commercial Taqman Gene Expression Assays were purchased from Applied Biosystems to determine the amount of GPR17 (Mm02619401_s1) and the housekeeping genes glyceraldehyde-3-phosphate dehydrogenase (Gapdh, Mm99999915_g1) and beta-actin (Actb, Mm00607939_s1). PCR amplifications were run in duplicate. Blank controls consisting in no template (water) or RT-negative reactions were performed for each run. Data extracted from each real time RT-PCR run were analysed by means of the 7000 v1.1 SDS instrument software (Applied Biosystems). A relative quantification approach was used, according to the 2^{-ddCT} method (Livak and Schmittgen, 2001). Suitable housekeeping genes were selected following Boda et al. (2009). On this basis, Gapdh was used for the quantifications of samples from cortical stab-wounds and controls, Actb for samples from APPPS1 and wild type mice.

Western Blot analysis

Brains from postnatal mice were extracted and rapidly frozen at -80°C. Membrane protein extracts were obtained by tissue homogenization in buffer A (50 mM Tris HCl, pH 7.4, 150 mM NaCl, 2mM EGTA and protease inhibitor cocktail, Sigma). The homogenate was centrifuged at

800 g for 10 min at 4°C, and the postnuclear supernatant was centrifuged at 200.000 g for 1 h at 4°C to generate membrane and cytosolic fractions. The membrane fractions were solubilised in buffer A containing 1% TritonX-100. The protein concentration was estimated using the Bio-Rad Protein Assay (Bio-Rad Laboratories s.r.l., Segrate, Italy). Western blot was performed as previously described (Taverna et al., 2004). Briefly, equal amounts of proteins (30 μg) for each sample were loaded on 10% SDS-PAGE and then blotted onto nitrocellulose filters (Invitrogen, San Giuliano Milanese, Italy). After blocking with 5% dry milk in TBS buffer (20 mM Tris pH 7.4, 150 mM NaCl), filters were probed with anti-GPR17 (1:1000), anti-Actin (mouse monoclonal 1:3000, Sigma) and anti-myelin associated glycoprotein (MAG) (mouse monoclonal 1:1000; Chemicon, Temecula, CA) antibodies diluted in TBS buffer containing 5% milk and 0.3% Tween 20. Aappropriate peroxidase-coupled secondary antibodies were applied for 1 hour at room temperature and peroxidase signals were detected using a chemiluminescent substrate (Pierce, Rockford, IL). Western blot analyses were run in triplicate.

Image processing and data analysis

Histological specimens were examined using an E-800 Nikon microscope (Nikon, Melville, NY) connected to a colour CCD Camera, a Leica TCS SP5 (Leica Microsystems, Wetzlar, Germany), or a Zeiss LSM710 (Carl Zeiss, Goettingen, Germany) confocal microscopes. All images were collected with the confocal microscope. Adobe Photoshop 6.0 (Adobe Systems, San Jose, CA) was used to adjust image contrast and assemble the final plates. Quantitative evaluations (cell densities, marker coexpression, soma diameters) were performed by confocal analysis or by means of the Neurolucida software (MicroBrightfield, Colchester, VT). Measurements derived from at least three sections per animal. Three to five animals were analysed for each time point or experimental condition. Routinely, a gray matter area (GM) of

11

about 500 μm^2 was evaluated together with the corresponding subcortical WM (see Supp. Info. Fig. 1B). WM was not analysed when confounding factors (i.e. proliferation of adjacent germinal areas; tightness of thin processes and high intensity of PLP/DM20 labelling) could affect the reliability of quantifications. For most markers, the number of inspected cells ranged from 100 to 700 cells per individual. In total, for BrdU (double pulse) and Ki67 staining at least 50-70 cells were analysed.

Soma diameters were calculated only for cells whose soma was entirely included in the confocal stack by averaging the values of their minimum and maximum diameters in two orthogonal directions (Kukley et al., 2010). Densitometric analysis of staining intensity and mapping of cell localization were made using ImageJ software (Research Service Branch, National Institutes of Health, Bethesda, MD; http://rsb.info.nih.gov/ij/). All quantifications were performed in the sensorimotor cortex (from -0.4 to -1.94 from bregma, Supp. Info. Fig. 1B). Statistical analyses were carried out by the SigmaStat software package (Jandel Scientific, Germany) and included one-way ANOVA test (to compare mean values) followed by Bonferroni's post-hoc analysis, unpaired Student's *t* test (when comparing only two groups), Fisher's exact text, Chi-square test or binomial test (to compare frequencies). Percentages were treated according to the arcsin transformation. In all instances, $P < 0.05$ was considered as statistically significant. Data were expressed as averages ± standard deviations.

RESULTS

Characterization of GPR17 expression in adult oligodendroglial cells

As an initial step of this study, we extended and detailed the first description of GPR17 expressing cells in the adult brain reported in Lecca et al. (2008). Consistent with these earlier findings, in the mature mouse cerebral cortex GPR17 antisera labelled some neurons (punctate somatic staining, arrows in Fig. 1D) and many other cells dispersed in the parenchyma. The non-neuronal cells were scattered in both GM (Fig. 1A) and WM (Fig. 1B) at a similar density (102.78 ± 26.18 cells/mm^2 and 114.18 ± 21.41 cells/mm^2 respectively, P=0.08) that remained quite stable over time during mouse ageing (cfr these data obtained in 2-4 month old animals and those for wild type mice in chronic amyloidosis analysis). Their oligodendroglial phenotype was confirmed by coexpression of the transcription factor Olig2 (see Supp. Info. Table 1, present in $93.57\pm3.44\%$ and $92.03\pm0.2\%$ of all GPR17+ cells in GM and WM, respectively; Fig. 1A-B'), and by the lack of costaining for microglial or astrocytic antigens (Iba1 and GFAP or S100β, respectively, data not shown). Furthermore, a careful confocal inspection revealed that in Olig2+ cells the GPR17 protein had distinct expression levels and cellular localisations. In about half of the cells ($56.8\pm5.6\%$ and $34.7\pm9.7\%$ in GM and WM, respectively), GPR17 protein was detected as a single intracellular spot (GPR17 protein, intracellular, henceforth mentioned as "Gpi" cells; arrows in Fig. 1A-B', C, arrowheads in Fig.1D,F',G; see also Lecca et al., 2008), corresponding mainly to the Golgi apparatus or also including the initial segments of 1-2 processes in tight contiguity with the Golgi pole (Fig. 1F,F'). Double staining analysis showed that these cells are distinct from GPR17-labelled neuron somata (Fig. 1D), and belong to multipolar oligodendrocyte precursors expressing NG2 (Stallcup, 2002) and PDGFRa (Nishiyama et al., 1996) (Fig.1C, G, L). NG2+ precursors displaying intracellular GPR17 protein were also found *in vitro* (Fig. 1E).

The rest of GPR17 positive cells exhibited a higher and broader GPR17 expression,

extended to both somata and processes and indicative of receptor localisation to the cell membrane (GPR17 receptor on cell membrane, henceforth mentioned as "Grm" cells; arrowheads in Fig. 1A-B'; H-K, M, N). Grm cells were proportionally more numerous among the GPR17+ population in the WM compared to GM (43.2±5.6% GM and 65.3±9.7 WM, $P<0.001$). Although lacking the precursor marker PDGFRa, about half of Grm cells still synthesised NG2 (Fig.1H-I', L: 46.62±22.90 % in GM; 43.82±9.09% in WM). As highlighted by detailed GM inspection, GPR17 labelling in processes was more prominent in cells with more complex morphologies (Fig. 1I) where, conversely, NG2 staining appeared reduced and discontinuous along ramifications, suggesting NG2 downregulation (Fig. 1H',I'). Interestingly, cells with highest receptor levels and broadest positive radiating processes were decorated for the immature proteolipid protein (PLP) splice variant PLP/DM20 (about 30% of Grm cells, GM; Kukley et al., 2010; Fig. 1J,L; and negative for the myelin protein PLP1, also detected by the AA3 antibody) and CD9 (Terada et al., 2002; Fig. 1K). Both PLP/DM20 and CD9 are well-known markers for premyelinating stages. Thus, Grm cells comprise both NG2+ elements and more mature premyelinating cells. This heterogeneity was also reflected in the range of cell soma sizes, comprising both small somata with diameters typical of PDGFRa precursors and a majority of larger cells with premyelinating features (Suppl. Fig. 2A,B; cfr also Kukley et al., 2010). Finally, Gpi and Grm cells together comprised about the 25% of the whole NG2+ cell population in both GM and WM (27.96 ± 7.59% and 22.3 ± 4.53%, respectively, P=0.114), demonstrating that GPR17 is translated in a relevant fraction of adult oligodendrocyte precursors. Accordingly, no colabelling was observed for GPR17 and markers for more mature or myelinating oligodendroglial stages such as glutathione S-transferase (GST)-π (Tamura et al., 2007; Fig. 1M), mature proteolipid protein (PLP1, Griffiths at al., 1998; Fig. 1N), 2',3'-cyclic nucleotide 3'-phosphodiesterase (RIP, Watanabe et al., 2006), myelin basic protein (MBP) and myelin

associated glycoprotein (MAG) (data not shown). On the whole, these data suggest that the Gpi and Grm staining patterns may represent different maturation stages of GPR17+ cells and that GPR17 can exert its receptor function in a fraction of adult NG2+ cells in transition to more mature stages and premyelinating oligodendrocytes.

GPR17 expression pattern during postnatal oligodendrocyte differentiation

With the aim to assess whether Gpi and Grm patterns constitute progressive phases of NG2+ cell maturation, we examined receptor expression during the first weeks of life. Similar to the adult brain, anti-GPR17 antibodies occasionally stained neurons (arrowheads in Fig. 2H, see also Fig. 3B and C) and clearly labelled Olig2+ cells (Fig. 2A-B'). The immunophenotype of these latter cells, as demonstrated by lack of coexpression of microglia- or astrocyte-specific markers (Iba1, GFAP, vimentin, data not shown), extensive overlap with NG2 (Fig. 2C), costaining for PDGFRa at low GPR17 expression levels (Fig. 2D), and absence of proteins typical for completed oligodendrocyte maturation (GST-π, PLP1, MAG and MBP, Fig. 2H-K), was consistent with that of adult GPR17+ cells.

GPR17+/Olig2+ cells were detected already at birth (Fig. 3A,E,F) and predominantly belonged to the Gpi type (Fig. 3A,H,I). During the first postnatal weeks, GPR17 expression was progressively increasing, as shown by the elevation in GPR17+ cell number between P0 and P7 (Fig. 3E,F) and by the enlargement of the Grm fraction, virtually absent at birth (Fig. 3H and I; P7-P14 vs. P0, $P<0.001$), indicating that the maturation of GPR17+ cells includes the switch from Gpi to Grm phenotypes. This interpretation was additionally strengthened by the observation that the distribution of GPR17 to cell ramifications recapitulated and anticipated the latero-medial and ventro-dorsal patterns of oligodendrocyte myelination in the cerebral cortex (Vincze et al., 2008; cfr Supp. Info. Fig. 3), although at earlier ages. Consistent with GPR17

upregulation during postnatal development, the fraction of GPR17 expressing cells among oligodendrocyte progenitors progressively increased (Fig.3G), and during the fourth postnatal week covered the vast majority of immature oligodendrocytes, identified either as Olig2+/Gst-π negative cells or as NG2+ cells (Fig. 3G, see also Fig. 4A). Interestingly, from P14, cells appeared that showed intense GPR17 positivity covering extended branches (Fig. 2E,G), as well as sparse processes aligning with axons or intercalating with the earliest myelin tracts (arrows in Fig. 2E,F,J,K), suggestive of premyelinating morphologies. Notably, these Grm cells often coexpressed PLP/DM20 and CD9 (Fig. 2E,G). Analysis of cortical GM at P24, showed that GPR17+/PLP/DM20+ cells covered about 60% of Grm cells (Fig. 4B). However, at this age NG2 was still coexpressed by the vast majority of GPR17+ cells, including both Gpi and Grm elements (Fig. 4A-B). These data imply some degree of overlap between NG2 and PLP/DM20 expression during postnatal differentiation (Fig. 4C, C'). Furthermore, in line with the adult phenotype and with different stages of maturation, Grm somata exhibited diameters typical of both oligodendrocyte precursors and premyelinating cells (Suppl. Info. Fig. 2).

Consistent with GPR17 anticipating myelination (see also Chen et al., 2009), massive myelin production followed the peak of GPR17+ cell density (P7-P14, Fig. 3A'-D' and Fig 3E, F) and occurred concomitantly with the decrease in GPR17+ cell number (Fig. 3D,D' and Fig. 3E,F). Western blot data confirmed these results (Fig. 3J). To explain the significant decrease in GPR17+ cell density in the progression to the mature stage (about 50% and 80% reduction in GM and WM, respectively; $P<0.05$, P24 vs. adult), possible signs of apoptosis in GPR17+ cells were evaluated by TUNEL assay and inspection of DAPI+ nuclei. Since we could not observe any positivity for DNA fragmentation or pyknosis (data not shown), the decline in GPR17+ cells is likely due to downregulation of the receptor during terminal differentiation. In summary, these data show that, similar to the adult pattern, GPR17 expression pertains to a fraction of postnatal

NG2+ cells in transition to maturity and that receptor expression is downregulated before the completion of myelin production.

Proliferative activity of GPR17-expressing cells in the adult and postnatal brain

One of the major and mostly debated traits of NG2+ cell heterogeneity is the capability to undergo cell proliferation (Bouslama-Oueghlani et al. 2005; Irvine and Blakemore, 2007; Rivers et al. 2008; Psachoulia et al., 2009; Simon et al., 2011). Considering the well-established role of GPR17 endogenous ligands (extracellular nucleotides, Ciana et al., 2006) as modulators of cell proliferation (Abbracchio et al., 1994; Agresti et al., 2005; Burnstock, 2006; Milosevic et al., 2006), we asked whether GPR17 expression could identify NG2+ cells endowed with a specific proliferative behaviour. To this aim, we applied diverse BrdU treatments to adult animals to analyse active mitosis (double pulse of the DNA base analogue BrdU followed by sacrifice, Suppl. Info Fig. 1A) or examine GPR17 + cell turnover (continuous administration of BrdU until sacrifice, Suppl. Info Fig. 1A) in comparison to NG2+ cells (see Material and Methods). In all cases, virtually all BrdU-incorporating cells were NG2+ (>80%).

When detecting cells undergoing or just exiting S-phase (BrdU double pulse protocol), only Gpi cells were decorated by BrdU staining while Grm cells were always negative (Fig. 5D,E). This observation was further confirmed by BrdU pulses at postnatal ages (P3, data not shown), and by labelling of the adult cortex for Ki67, a marker for active divisions (Taupin, 2007). The Gpi fractions among BrdU+ cells (22.35±7.45% in GM, 11.71±3.12% in WM, Fig. 5D,E) were overall in line with the corresponding Gpi proportions amongst NG2+ cells (19.31 ±5.6% in GM, 13.21±6.7% in WM; $P>0.05$). Consistently, the proliferative fractions of Gpi cells (2.27±1.29% in GM; 7.26±2.60% in WM) were similar to that of NG2+ cells (1.90±0.65% in GM; 8.36±2.00% in WM; $P>0.05$). Moreover, among Ki67+/NG2+ cells, 22.11±8.64% expressed the

GPR17 protein in the GM (Fig. 5D), while virtually none (1.13±2.27%) was positive in the WM (Fig. 5E). Thus, Gpi cells can undergo active proliferation and behave similarly to NG2+ precursors. The discrepancy between GM and WM highlighted also by the difference between the total number of BrdU+ and Ki67+ cells in these regions (Fig5 D, E), points to distinct cell cycle length and maturation speed in these territories (Dimou et al 2008; Kang et al 2010).

When long BrdU administration was applied, one day after starting the BrdU treatment, the proliferative proportion of GPR17-expressing cells was about 3 fold lower than that of NG2+ cells (Fig. 5A and B; $P<0.05$ in both GM and WM). Nevertheless, at later time points, this difference disappeared (Fig. 5A and B, $P>0.05$), thereby ruling out the possibility of a slower proliferation rate for the whole GPR17+ pool, and rather suggesting GPR17 upregulation over time in newly-generated cells. Notably, BrdU+/GPR17+ cells progressively increased in number and included the vast majority of GPR17+ cells within about one-month of treatment (14 days, GM, 31.33±8.72%, WM, 45.86±5.3%; 28 days, GM, 64.62±2.56%, WM, 77.14±12.06%), underlying that GPR17+ cells undergo a continuous turn over with rates similar to that of all NG2+ cells (present work and Simon et al., 2011). Furthermore, while at short times after cumulative BrdU treatment almost all GPR17+/BrdU+ cells belonged to the Gpi type (92.5±17.53% at 1 day), with longer exposures the receptor was also expressed in cell ramifications (Fig. 5F,L), consistent with a progressive upregulation of the receptor after division. In summary, GPR17 is induced in NG2+ cells by the end of the cell cycle and its upregulation defines a stage when cells are non-proliferative.

Timing and pattern of GPR17 induction in adult and postnatal newly generated NG2+ cells

Because the previous analysis suggested an upregulation of the receptor after proliferation, we performed BrdU-based label retaining experiments to examine the precise timing of GPR17 induction in newly generated NG2+ cells. In a first set of experiments, a synchronized pool of newborn cells labelled by a double BrdU pulse (Supp. Info. Fig. 1A) was followed over time. The fractions of GPR17+/BrdU+ cells expanded to about half of all newborn cells by 4-7 dpi (4dpi 56.69±8.73% and 36.96±5.09%, 7dpi 52.01±2.46% and 39.14±4.59% in GM and WM, respectively, Fig. 5H and I) but never covered the entire BrdU-tagged population. In both GM and WM, the double-positive fractions declined at later time points and WM cells exhibited a faster kinetic (about 45% decline between 4 and 7dpi vs. 60% decline in GM only after 7dpi). In WM this reduction was accompanied by a decrease in the absolute number of BrdU+ cells, again suggesting a major propensity of WM cells to undergo multiple divisions and therefore to dilute out the incorporated BrdU (Dimou et al., 2008; Kang et al. 2010). In agreement with the pattern of postnatal ontogenesis, while at 1 dpi virtually all the newly generated GPR17+ cells were Gpi, at 4 and 7 dpi Grm cells with strong and spread receptor expression covered a relevant fraction (4 dpi, 35.26±5.7% and 57.41±15.3%; 7 dpi, 32.78±7.52% and 57.78±6.71% in GM and WM, respectively). Further on, the Grm proportions diminished again (13.03±10.57% and 23.81±13.47% in GM and WM, respectively), confirming the transient expression of the receptor and the maintenance of GPR17 for long times only in a small cell pool. Similar data were also obtained when GPR17 regulation was examined in newly produced oligodendrocyte precursor of the immature cortex (Supp. Info. Fig. 4). Again, GPR17 did not appear in all GM BrdU+ cells, and was transiently regulated.

The BrdU treatment employed so far labelled cells capable of DNA duplication within few hours (fast dividing cells) that appeared rather rare in the adult parenchyma (Fig. 5D,E). Nonetheless, adult NG2+ cells likely comprise cells with longer cell cycle lengths. To include

these cells, we tagged both fast and slow proliferating cells by administering BrdU for two weeks (Supp. Info. Fig 1A) and evaluated the fate of BrdU-incorporating cells (virtually all were NG2+, see Simon et al., 2011) in terms of GPR17 expression at the end of treatment and up to 10 weeks after. While the total number of GPR17+ cells remained stable over time (not shown, see also above), GPR17+/BrdU+ cells increased during the first 2 weeks of retaining in the GM (Fig. 5J,K), further supporting the hypothesis that the receptor is induced after proliferation. In the WM, this early induction was not appreciable, likely because it was masked by both a fast receptor decline and a prompt differentiation to mature oligodendrocytes (see double BrdU pulse data and below). The double+ cells were then decreasing in both GM and WM (see also Fig. 5F,G and L, M), consistent with progression to differentiation. Interestingly, and in agreement with previous data, in the WM the decline in the number of double+ cells after 2 weeks retaining was more pronounced compared to GM (Fig. 5J,K and F,G,L,M), supporting the notion of distinct differentiation properties of GM and WM NG2+ cells (Dimou et al., 2008; Kang et al., 2010). In addition, and in agreement with the short BrdU pulse data, the fraction of double+ cells among all BrdU+ cells never reached 100% in both GM and WM (Fig. 5J and K).

On the whole, these data indicate that GPR17 upregulation occurs early after mitosis and that, within the time limits of our analysis, pertains only to a subset of NG2+ cells. Furthermore, they show that GPR17 expression is transitory, and that receptor expression is regulated according to distinct kinetics in GM and WM.

GPR17+ cells participate in the parenchymal response to traumatic injury

The emerging role of endogenous nucleotides as danger signals upon brain and spinal cord injury (Wang et al., 2004; Davalos et al., 2005; Haynes et al., 2006), has raised the hypothesis that GPR17 responding to extracellular nucleotides and cysteinyl-leukotrienes may act as a

crucial mediator of NG2+ cell reactivity (Hampton et al., 2004, Simon et al., 2011) to acute injury such as ~~acute~~ cortical trauma (stab-wound, SW).

After SW, GPR17+ cells maintained their phenotype as shown by Olig2 and NG2 coexpression and absence of mature oligodendroglial markers or GFAP costaining (data not shown). At variance with what occurred in other CNS injury models (Lecca et al., 2008; Ceruti et al., 2009), after SW GPR17 was neither detected in Iba1+ microglial cells nor was found in round-shaped NG2+ blood-derived macrophages (data not shown, see Hampton et al., 2004) or in NG2+ pericytes. At 1 day post lesion (dpl) the density of GM GPR17+ oligodendroglial cells was reduced to one fourth of the value of the contralateral cortex (Fig. 6B,E; $P<0.05$), which was similar to that of intact mice ($P>0.05$). This decrease was accompanied by significant reduction in the Grm proportion (Fig. 6F, about 30% less than controls; $P<0.01$), and the GPR17 fraction amongst NG2+ cells (7.97 ± 0.96 %; $P<0.001$), whose density was unchanged (Fig. 6E). Conversely, the density of GPR17+ cells did not change shortly after lesion in the WM (Fig. 6H), once more underlying distinct properties of GM/WM cells. At later time points, GPR17+ cells increased significantly in number around the lesion in both GM and WM, consistently with the expansion of NG2+ pool (Fig. 6C, E, H). This reactivity lasted up to 7 days and then declined over time, going back to basal levels at 14 dpl, when, conversely, NG2+ cell density was still increased (Fig. 6E and H). The time-dependent pattern of receptor expression revealed by immunohistochemical analysis was confirmed by quantitative evaluation of GPR17 mRNA in the lesioned cortex (Supp. Info Fig. 5A).

To substantiate the evidence for a post-acute GPR17 upregulation after SW, we found that the GM Grm fraction significantly exceeded control values between 4 and 14 dpl (Fig. 6F; $P<0.001$). Conversely, this did not occur in the WM (Fig. 6I). Interestingly, the pattern of Grm expansion displayed a specific spatio-temporal distribution: while Gpi cells increased in density

close to the lesion site at 4 dpl, Grm cells remained mostly located far away from the lesion

(250-300 μm) and appeared closer to the SW only at later time points (Supp. Info Fig. 6). This

observation likely reflects a distal-to proximal wave of NG2+ cell maturation.

Finally, we assessed whether GPR17+ cells, although being reduced in number early

after lesion, might specifically contribute to NG2+ cell reactivity with intense proliferative activity.

At short times after BrdU administration, dividing GPR17+ cells exclusively belonged to the Gpi

type, as also observed in the intact brain. Moreover, at 1 day after BrdU cumulative treatment

(dpt) the GPR17+ proliferative fraction remained lower than that of NG2+ cells (Fig. 6G;

P=0.028) in GM, while in WM it reached the levels of NG2+ cells (Fig. 6J; P>0.05). Afterwards,

as it was the case in the intact cortex, BrdU incorporation into GPR17+ and NG2+ cells was

almost equivalent (P>0.05), showing that about 80% of both cell types had been generated "de

novo" over the examined time window (Fig. 6G and J). Thus, the presence of GPR17 does not

define a NG2+ cell subset capable to trigger and sustain NG2+ cell reaction to acute lesion by

GPR17 upregulation or proliferation. Rather, receptor induction takes part in the post-acute

response to damage according to a pattern reminiscent of GPR17 expression during

oligodendroglia ontogenesis.

 GPR17+ cells participate in the parenchymal response to chronic amyloidosis

To study the possible contribution of GPR17 expressing cells to the parenchymal response to a

chronic injury, we investigated its expression in the APPPS1 mouse, a transgenic model of

Alzheimer's Disease (Buffo et al., 2005; Radde et al., 2006). Also in this lesion condition,

GPR17 staining was never observed in GFAP+ astrocytes (data not shown), Iba1+ microglial

cells, or in mature oligodendrocytes (data not shown). Notably, GPR17+/Olig2+ cells increased

significantly in number in the APPPS1 cortical GM (Fig. 7B and C; P<0.05) compared to age-

matched WT animals. However, the fraction of GM NG2+ cells coexpressing the receptor in APPPS1 cortices (28.17±2.85%) remained similar to that of WT mice (29.76±5.79%). On the contrary, GPR17+ cell density was unchanged in the underlying WM (123.34±10.55 cells/mm^2 APPPS1; 128.72±27.08 cells/mm^2 WT), where β-amyloid plaques are less abundant, indicating a specific correlation between amyloid aggregates and the increase in the GPR17+ cell number. In the GM most GPR17+ cells (64.51±4.01%) clustered in close proximity of β-amyloid plaques (within 50 μm from the plaque border; Fig. 7B,B'), where also Iba1+ microglial cells accumulated (Fig. 7B'). Here, the majority of GPR17+ cells (74.39±13.28% vs. 43.2±5.6% of controls, *P*<0.001) displayed a strong receptor labelling along the whole cell body and processes (Grm type; Fig. 7D), further supporting the correlation between GPR17 induction and plaques. Yet, no significant upregulation of the GPR17 mRNA content was found in APPPS1 cortex (Supp. Info Fig. 5B), suggesting a modulation at the level of translation or of the stability of GPR17 protein.

When proliferation of GPR17+ cells was analysed after a 7 day-long administration of BrdU (Fig. 7E), we found a distinct behaviour for GPR17+ and NG2+ cells in the APPPS1 cortical GM. While the NG2+ cell population maintained its rate of division, the fraction of BrdU-labelled GPR17 expressing cells was significantly higher in the APPPS1 cortex than that in wild type mice (Fig. 7E; P<0.001). However, even in this condition, actively dividing cells labelled by means of two subsequent BrdU injections belonged to the Gpi type, whereas Grm cells never incorporated BrdU (not shown). Moreover, the proliferative fraction of GPR17 expressing cells remained similar to that of wild type animals (1.52±0.77% in APPPS1, 1.28±0.72% in WT, after a double BrdU pulse). Thus, the increase in the GPR17+ proliferative fraction, rather than reflecting an enhanced active proliferation, is consistent with an anticipated induction of the receptor in newly generated cells and/or with its maintenance for longer times. On the whole, these data reveal that the upregulation of GPR17 is a hallmark of reactivity to cerebral

amyloidosis.

DISCUSSION

To shed light on the heterogeneity and antigenic indistinguishability of NG2+ cells, we examined the expression pattern of the newly identified oligodendroglial GPR17 receptor in the intact mouse cerebral cortex at mature and developmental stages, and in conditions of traumatic injury and chronic amyloidosis. We show that in the adult and early postnatal cortex NG2+ cells progressively upregulate GPR17 after cell division until they reach the premyelinating stage. GPR17 downregulation, occurring with distinct kinetics in gray and white matter, coincides with further differentiation of cells and expression of myelin proteins (Table 1). During postnatal ontogenesis, GPR17 appearance anticipates the major myelination phase and decorates a proportion of oligodendroglial precursors initially expanding within the first month of life, and then decreasing as the tissue matures. GPR17 induction also participates in the response to traumatic injuries at post-acute stages and to chronic pathology.

GPR17 in NG2+ cell diversity and maturation

NG2-expressing cells display heterogeneous functional and phenotypical characteristics in distinct CNS territories, upon lesion or during ageing (Gilson and Blakemore, 1993; Levine et al., 1993; Hampton et al., 2004; Dimou et al., 2008; Rivers et al., 2008; Irvine and Blakemore, 2007; Simon et al., 2011). While both extrinsic environmental cues and intrinsic factors have been proposed to explain such variability (Hampton et al, 2004; Dimou et al., 2008; Lytle et al., 2009; Nishiyama et al, 2009), the molecular substrates discriminating specific functional competences or distinct maturation stages among NG2+ cells remain essentially unidentified. Our study reveals that diverse GPR17 expression levels and compartmentalization identify

defined oligodendroglial statuses. Indeed, low expression and intracellular localisation of GPR17 protein, indicative of the early activation of its biosynthetic pathway, correspond to NG2+ cells in mitosis, or that just exited mitosis. Conversely, high GPR17 levels in both perikarium and processes and its localisation on the cell membrane define a more mature and non-proliferative stage of oligodendroglial cells. Further, intense GPR17 expression accompanies these cells until the premyelinating stage. On the whole, these results point to GPR17 induction as a marker of maturation of NG2+ cells in transition from precursor to premyelinating phenotypes. These data also suggest that the GPR17 receptor exerts its function of detector of extrinsic signals in post-mitotic NG2+ cells and premyelinating oligodendrocytes, and clarify that, given its intracellular localisation, it cannot act in that way in proliferative NG2+/PDGFRa+ precursors.

Notably, however, GPR17 induction characterizes only about one third of the progeny of the cycling NG2+ pool, meaning that that diverse progenitor subsets exist with distinct molecular mechanisms to sense the environment and regulate their fate. While intracellular GRP17 protein does not confer specific proliferative capabilities to NG2+ cells, exposure of the receptor to the cell membrane coincides with non-mitotic stages, in line with their commitment to differentiation. This finding suggests that receptor positive and negative progenies may have diverse differentiation capabilities. GPR17-mediated signals have been proposed to be required for receptor downregulation and further cell maturation (Lecca et al., 2008; Fumagalli et al., 2011; E. Parmigiani et al., unpublished). Our *in vivo* data on receptor downregulation before expression of myelin proteins are in line with these results and also highlight a function of GPR17 in the acquisition of premyelinating traits. Nevertheless, while we clearly proved that GPR17 expressing cells are engaged in differentiation (at least until the premyelinating stage), we have no elements to infer whether receptor negative NG2+ cells remain immature or

differentiate. The early appearance of mature and myelinating oligodendrocytes in the first weeks of postnatal life, occurring well before the decrease in GPR17+ cell numbers (Fig. 3E,F), suggests that receptor negative cells are also able to progress to differentiation. However, the broader GPR17 distribution to cell processes in the adult WM compared to GM and the faster receptor downregulation in WM cells compared to GM ones well correlate with more efficient myelination capabilities in this territory (Dimou et al., 2008), consistently with GPR17 induction, signalling and downregulation being crucial for maturation of NG2+ cells to oligodendrocytes (Lecca et al., 2008; Chen et al., 2009; Fumagalli et al., 2011). Yet, only cell tracking experiments of GPR17-positive/negative cells will resolve the issue of distinct differentiation capabilities of negative and positive pools. Similarly, only pharmacological studies with GPR17-selective compounds in native systems will disclose the exact mechanisms of GPR17 functioning.

Regulation of GPR17 expression

The existence of GPR17-positive and negative NG2+ cells brings up the issues of the lineage relationships between these cell subsets and of the mechanisms regulating GPR17 expression. The finding that GPR17+/NG2+ cells can derive from receptor-negative mitotic cells suggests that the two subsets do not belong to separate clones. Moreover, the correspondence between the timing of GPR17 appearance during postnatal development and the pattern of oligodendrocyte maturation strongly points to the existence of an intrinsic activation program for GPR17 expression, appearing thus as a default event, at least in the lineage of an oligodendrocyte subset. Distinct progenitor populations originating either in the ventral or dorsal forebrain ventricular zones have been described to contribute to embryonic, postnatal and adult cortical oligodendroglia (Kessaris et al., 2006). Whether intrinsic

determinants encoded in these forebrain progenitor populations account for receptor-positive and -negative pools is not known. Despite ventral and dorsal oligodendroglia cells have been shown to share several features (electrical properties, number of wrapped axons, neurotransmitter receptor responses, Tripathi et al., 2011), in future studies it will be interesting to examine whether GPR17 differentially pertains to these populations. However, Lecca and coworkers (2008) also demonstrated that, besides stimulating differentiation, GPR17 endogenous ligands also directly affect GPR17 expression, thus pointing to an extrinsic time- and regional-specific activation program for receptor induction. Indeed, uracyl nucleotides and their glycosylated derivatives are released not only in lesion conditions but also in the intact parenchyma (Lecca and Ceruti 2008), therefore potentially contributing to GPR17 physiological regulation. Our study further suggests that signals associated to β-amyloid plaques participate in inducing and/or maintaining high levels of receptor expression. Such signals may derive from dystrophic (Wirths et al., 2007), demyelinated or dysmyelinated axons (Desai et al., 2009; G. Behrendt, unpublished) and/or from activated microglia (Radde et al., 2006). Similarly, signals acutely released at the site of traumatic lesion modulate GPR17 synthesis. In fact, early after stab-wound receptor expression is downregulated in NG2+ cells. Notably, such changes do not occur in the damaged WM, underscoring once again the different features of gray and white matter territories. Growth factors appear as possible candidates for GM downregulation, because they take part in the tissue reaction to injury (Buffo et al., 2010) and have been shown to dampen GPR17 expression in oligodendrocyte precursors *in vitro* (Ceruti et al., 2011).

GPR17 expressing cells in injury

While former reports indicated that receptor activity mediates acute neuronal and myelin vulnerability to ischemic and traumatic injury (Ciana et al., 2006, Lecca et al, 2008; Ceruti et al., 2009), here we clarify that GPR17 neither is upregulated in NG2+ progenitors as part of their early reactivity, nor receptor activity triggers an increased proliferative response in positive cells. Conversely, GPR17 induction takes place at post-acute stages of tissue remodelling and recapitulates the ontogenetic pattern of receptor expression. In agreement with these data, ~~Notably,~~GPR17+ cells do not activate rapid proliferation in chronic cerebral amyloidosis and accumulate close to plaques, revealing receptor induction ~~GPR17 upregulation contributes also to the tissue response to cerebral amyloidosis and appears~~ as an additional feature of oligodendroglial reactivity in this pathology (Buffo et al., 2005). Our data indicate that the timing of GPR17 appearance in oligodendrocyte progenitors reacting to lesion likely reflects newborn cell maturation, and may correlate with regenerative attempts directed at repairing oligodendrocyte damage occurring under these injury conditions (Lotocki et al., 2011; Mitew et al., 2010; Desai et al., 2009). However, receptor overexpression was also described in an immune-mediated model of~~conditions~~ chronic demyelination, where recurrent myelin damage is not compensated by NG2+ cell reparative responses, supporting the interpretation of GPR17 as a factor hampering of myelin restoration ~~(Chen at al., 2009)~~. Yet, we found a strong GPR17 induction in a focal demyelination model (Supp. Info Fig. 7), where spontaneous recovery normally occurs (Woodruff and Franklin, 1999; Birgbauer et al., 2004). Notably, also in this case GPR17+ cells accrued at sites of demyelination at post-acute stages, in a time window corresponding to the initiation of oligodendrocyte repair (Woodruff and Franklin, 1999). These data would rather support a function for the receptor in myelin reconstitution. ~~Contrary to a prominent role of GPR17+ cells in the failure of myelin restoration, we found a strong GPR17 induction in a focal demyelination model (Supp. Info. Fig. 7), where~~

~~spontaneous recovery normally occurs (Woodruff and Franklin, 1999; Birgbauer et al., 2004).~~ To tentatively reconcile these different interpretations, it may be hypothesized that GPR17 induction reflects an initial attempt to start re-myelination, but that its dysregulated sustained over-expression at late oligodendroglial maturation stages as a result of the local inflammatory microenvironment turns an initial beneficial reaction into a detrimental one. Thus, given the massive presence of GPR17 in oligodendrocyte progenitors during post-acute reactivity to various injury conditions, with diverse extent of oligodendrocyte damage and reparative outcomes, it will be crucial to understand whether and how ~~These findings strengthen the possibility that appropriate pharmacological~~ manipulations of GPR17 may potentiate manipulations of GPR17 may potentiate reparative myelination ~~in various pathological conditions~~.

Acknowledgments

References

Abbracchio MP, Saffrey MJ, Höpker V, Burnstock G.1994. Modulation of astroglial cell proliferation by analogues of adenosine and ATP in primary cultures of rat striatum. Neuroscience 59:67-76.

Agresti C, Meomartini ME, Amadio S, Ambrosini E, Serafini B, Franchini L, Volonte C, Aloisi F, Visentin S. 2005. Metabotropic P2 receptor activation regulates oligodendrocyte progenitor migration and development. Glia 50:132-144.

Bakiri Y, Attwell D, Karadottir R. 2009. Electrical signalling properties of oligodendrocyte precursor cells. Neuron Glia Biol 5:3-11.

Birgbauer E, Rao TS, Webb M. 2004. Lysolecithin induces demyelination in vitro in a cerebellar slice culture system. J Neurosci Res 78:157-166.

Boda E, Buffo A. 2010. Glial cells in non-germinal territories: insights into their stem/progenitor properties in the intact and injured nervous tissue. Arch Ital Biol 148:119-136.

Boda E, Pini A, Hoxha E, Parolisi R, Tempia F. 2009. Selection of reference genes for quantitative real-time RT-PCR studies in mouse brain. J Mol Neurosci 37:238-253.

Bouslama-Oueghlani L, Wehrle R, Sotelo C, Dusart I. 2005. Heterogeneity of NG2-expressing cells in the newborn mouse cerebellum. Dev Biol 285:409-421.

Buffo A, Rolando C, Ceruti S. 2010. Astrocytes in the damaged brain: molecular and cellular insights into their reactive response and healing potential. Biochem Pharmacol 79:77-89.

Buffo A, Vosko MR, Erturk D, Hamann GF, Jucker M, Rowitch D, Gotz M. 2005. Expression pattern of the transcription factor Olig2 in response to brain injuries: implications for neuronal repair. Proc Natl Acad Sci U S A 102:18183-18188.

Burnstock G. 2006. Purinergic signalling. Br J Pharmacol 147 Suppl 1:S172-181.

Butt AM, Kiff J, Hubbard P, Berry M. 2002. Synantocytes: new functions for novel NG2

expressing glia. J Neurocytol 31:551-565.

Ceruti S, Villa G, Genovese T, Mazzon E, Longhi R, Rosa P, Bramanti P, Cuzzocrea S, Abbracchio MP. 2009. The P2Y-like receptor GPR17 as a sensor of damage and a new potential target in spinal cord injury. Brain 132:2206-2218.

Ceruti S, Viganò F, Boda E, Ferrario S, Magni G, Rosa P, Buffo A, Abbracchio MP. 2011. Expression of the new P2Y-like receptor GPR17 during oligodendrocyte precursor cell maturation regulates sensitivity to ATP-induced death. Glia 59: 363-378.

Chen Y, Wu H, Wang S, Koito H, Li J, Ye F, Hoang J, Escobar SS, Gow A, Arnett HA, Trapp BD, Karandikar NJ, Hsieh J, Lu QR. 2009. The oligodendrocyte-specific G protein-coupled receptor GPR17 is a cell-intrinsic timer of myelination. Nat Neurosci 12:1398-1406.

Ciana P, Fumagalli M, Trincavelli ML, Verderio C, Rosa P, Lecca D, Ferrario S, Parravicini C, Capra V, Gelosa P, Guerrini U, Belcredito S, Cimino M, Sironi L, Tremoli E, Rovati GE, Martini C, Abbracchio MP. 2006. The orphan receptor GPR17 identified as a new dual uracil nucleotides/cysteinyl-leukotrienes receptor. EMBO J 25:4615-4627.

Ciceri P, Rabuffetti M, Monopoli A, Nicosia S. 2001. Production of leukotrienes in a model of focal cerebral ischaemia in the rat. Br J Pharmacol 133:1323-1329.

Davalos D, Grutzendler J, Yang G, Kim JV, Zuo Y, Jung S, Littman DR, Dustin ML, Gan WB. 2005. ATP mediates rapid microglial response to local brain injury in vivo. Nat Neurosci 8:752-758.

Dawson MR, Polito A, Levine JM, Reynolds R. 2003. NG2-expressing glial progenitor cells: an abundant and widespread population of cycling cells in the adult rat CNS. Mol Cell Neurosci. 24:476-88.

De Biase LM, Nishiyama A, Bergles DE. 2010. Excitability and synaptic communication within the oligodendrocyte lineage. J Neurosci 30:3600-3611.

Desai MK, Sudol KL, Janelsins MC, Mastrangelo MA, Frazer ME, Bowers WJ. 2009. Triple-transgenic Alzheimer's disease mice exhibit region-specific abnormalities. Glia 57:54-65.

Dimou L, Simon C, Kirchhoff F, Takebayashi H, Gotz M. 2008. Progeny of Olig2-expressing progenitors in the gray and white matter of the adult mouse cerebral cortex. J Neurosci 28:10434-10442.

Fumagalli M, Daniele S, Lecca D, Lee PR, Parravicini C, Fields RD, Rosa P, Antonucci F, Verderio C, Trincavelli ML, Bramanti P, Martini C, Abbracchio MP. 2011. Phenotypic changes, signaling pathway, and functional correlates of GPR17-expressing neural precursor cells during oligodendrocyte differentiation. J Biol Chem 286:10593-10604.

Gilson J, Blakemore WF. 1993. Failure of remyelination in areas of demyelination produced in the spinal cord of old rats. Neuropathol Appl Neurobiol 19:173-181.

Griffiths I, Klugmann M, Anderson T, Thomson C, Vouyiouklis D, Nave KA. 1998 Current concepts of PLP and its role in the nervous system. Microsc Res Tech 41:344-358.

Hampton DW, Rhodes KE, Zhao C, Franklin RJ, Fawcett JW. 2004. The responses of oligodendrocyte precursor cells, astrocytes and microglia to a cortical stab injury, in the brain. Neuroscience 127:813-820.

Haynes SE, Hollopeter G, Yang G, Kurpius D, Dailey ME, Gan WB, Julius D. 2006. The P2Y12 receptor regulates microglial activation by extracellular nucleotides. Nat Neurosci 9:1512-1519.

Horner PJ, Power AE, Kempermann G, Kuhn HG, Palmer TD, Winkler J, Thal LJ, Gage FH. 2000. Proliferation and differentiation of progenitor cells throughout the intact adult rat spinal cord. J Neurosci 20:2218-2228.

Irvine KA, Blakemore WF. 2007. A different regional response by mouse oligodendrocyte progenitor cells (OPCs) to high-dose X-irradiation has consequences for repopulating OPC-

depleted normal tissue. Eur J Neurosci 25:417-424.

Jung M, Kramer E, Grzenkowski M, Tang K, Blakemore W, Aguzzi A, Khazaie K, Chlichlia K, von Blankenfeld G, Kettenmann H, et al. 1995. Lines of murine oligodendroglial precursor cells immortalized by an activated neu tyrosine kinase show distinct degrees of interaction with axons in vitro and in vivo. Eur J Neurosci 7:1245-1265.

Kang SH, Fukaya M, Yang JK, Rothstein JD, Bergles DE. 2010. NG2+ CNS glial progenitors remain committed to the oligodendrocyte lineage in postnatal life and following neurodegeneration. Neuron 68:668-81.

Kessaris N, Fogarty M, Iannarelli P, Grist M, Wegner M, Richardson WD. 2006. Competing waves of oligodendrocytes in the forebrain and postnatal elimination of an embryonic lineage. Nat Neurosci 9:173-179.

Kukley M, Nishiyama A, Dietrich D. 2010. The fate of synaptic input to NG2 glial cells: neurons specifically downregulate transmitter release onto differentiating oligodendroglial cells. J Neurosci 30:8320-8331.

Lecca D, Ceruti S. 2008. Uracil nucleotides: from metabolic intermediates to neuroprotection and neuroinflammation. Biochem Pharmacol 75:1869-1881.

Lecca D, Trincavelli ML, Gelosa P, Sironi L, Ciana P, Fumagalli M, Villa G, Verderio C, Grumelli C, Guerrini U, Tremoli E, Rosa P, Cuboni S, Martini C, Buffo A, Cimino M, Abbracchio MP. 2008. The recently identified P2Y-like receptor GPR17 is a sensor of brain damage and a new target for brain repair. PLoS One 3:e3579.

Levine JM, Stincone F, Lee YS. 1993. Development and differentiation of glial precursor cells in the rat cerebellum. Glia 7:307-321.

Livak KJ, Schmittgen TD. 2001. Analysis of relative gene expression data using real-time quantitative PCR and the 2(-Delta Delta C(T)) Method. Methods 25:402-408.

Lotocki G, Vaccari, Jde R, Alonso O, Molano JS, Nixon R, Safavi P, Dietrich WD, Bramlett HM. 2011 Oligodendrocyte vulnerability following traumatic brain injury in rats. Neurosci Lett. 499:143-148.

Lytle JM, Chittajallu R, Wrathall JR, Gallo V. 2009. NG2 cell response in the CNP-EGFP mouse after contusive spinal cord injury. Glia 57:270-285.

Melani A, Turchi D, Vannucchi MG, Cipriani S, Gianfriddo M, Pedata F. 2005. ATP extracellular concentrations are increased in the rat striatum during in vivo ischemia. Neurochem Int 47:442-448.

Milosevic J, Brandt A, Roemuss U, Arnold A, Wegner F, Schwarz SC, Storch A, Zimmermann H, Schwarz J. 2006. Uracil nucleotides stimulate human neural precursor cell proliferation and dopaminergic differentiation: involvement of MEK/ERK signalling. J Neurochem 99:913-923.

Mitew S, Kirkcaldie MT, Shepard CE, Vickers JC, Dickson TC. 2010 Focal demyelination in Alzheimer's disease and transgenic mouse models. Acta Neuropathol. 119:567-577.

Nishiyama A, Lin XH, Giese N, Heldin CH, Stallcup WB. 1996. Co-localization of NG2 proteoglycan and PDGF alpha-receptor on O2A progenitor cells in the developing rat brain. J Neurosci Res 43:299-314.

Nishiyama A, Watanabe M, Yang Z, Bu J. 2002. Identity, distribution, and development of polydendrocytes: NG2-expressing glial cells. J Neurocytol 31:437-455.

Nishiyama A, Komitova M, Suzuki R, Zhu X. 2009. Polydendrocytes (NG2 cells): multifunctional cells with lineage plasticity. Nat Rev Neurosci 10:9-22.

Psachoulia K, Jamen F, Young KM, Richardson WD. 2009. Cell cycle dynamics of NG2 cells in the postnatal and ageing brain. Neuron Glia Biol 5:57-67.

Pugliese AM, Trincavelli ML, Lecca D, Coppi E, Fumagalli M, Ferrario S, Failli P, Daniele S,

35

Martini C, Pedata F, Abbracchio MP. 2009. Functional characterization of two isoforms of the P2Y-like receptor GPR17: [35S]GTPgammaS binding and electrophysiological studies in 1321N1 cells. Am J Physiol Cell Physiol 297:C1028-1040.

Radde R, Bolmont T, Kaeser SA, Coomaraswamy J, Lindau D, Stoltze L, Calhoun ME, Jaggi F, Wolburg H, Gengler S, Haass C, Ghetti B, Czech C, Holscher C, Mathews PM, Jucker M. 2006. Abeta42-driven cerebral amyloidosis in transgenic mice reveals early and robust pathology. EMBO Rep 7:940-946.

Rivers LE, Young KM, Rizzi M, Jamen F, Psachoulia K, Wade A, Kessaris N, Richardson WD. 2008. PDGFRA/NG2 glia generate myelinating oligodendrocytes and piriform projection neurons in adult mice. Nat Neurosci 11:1392-1401.

Simon C, Götz M, Dimou L. (2011) Progenitors in the adult cerebral cortex: Cell cycle properties and regulation by physiological stimuli and injury. Glia 59:869-881. Stallcup WB. 2002. The NG2 proteoglycan: past insights and future prospects. J Neurocytol 31:423-435.

Tamura Y, Kataoka Y, Cui Y, Takamori Y, Watanabe Y, Yamada H. 2007. Intracellular translocation of glutathione S-transferase pi during oligodendrocyte differentiation in adult rat cerebral cortex in vivo. Neuroscience 148:535-540.

Taupin P. 2007. BrdU immunohistochemistry for studying adult neurogenesis: paradigms, pitfalls, limitations, and validation. Brain Res Rev. 53:198-214.

Taverna E, Saba E, Rowe J, Francolini M, Clementi F, Rosa P. 2004. Role of lipid microdomains in P/Q-type calcium channel (Cav2.1) clustering and function in presynaptic membranes. J Biol Chem 279:5127-5134.Terada N, Baracskay K, Kinter M, Melrose S, Brophy PJ, Boucheix C, Bjartmar C, Kidd G, Trapp BD. 2002. The tetraspanin protein, CD9, is expressed by progenitor cells committed to oligodendrogenesis and is linked to beta1 integrin, CD81, and Tspan-2. Glia 40:350-359.

Tripathi RB, Clarke LE, Burzomato V, Kessaris N, Anderson PN, Attwell D and William D. Richardson WD. 2011. Dorsally and Ventrally Derived Oligodendrocytes Have Similar Electrical Properties but Myelinate Preferred Tracts J Neurosci 31:6809–6819.

Trotter J, Karram K, Nishiyama A. 2010. NG2 cells: Properties, progeny and origin. Brain Res Rev 63:72-82.

Vincze A, Mazlo M, Seress L, Komoly S, Abraham H. 2008. A correlative light and electron microscopic study of postnatal myelination in the murine corpus callosum. Int J Dev Neurosci 26:575-584.

Wang X, Arcuino G, Takano T, Lin J, Peng WG, Wan P, Li P, Xu Q, Liu QS, Goldman SA, Nedergaard M. 2004. P2X7 receptor inhibition improves recovery after spinal cord injury. Nat Med 10:821-827.

Watanabe M, Sakurai Y, Ichinose T, Aikawa Y, Kotani M, Itoh K. 2006. Monoclonal antibody Rip specifically recognizes 2',3'-cyclic nucleotide 3'-phosphodiesterase in oligodendrocytes. J Neurosci Res 84:525-533.

Wirths O, Weis J, Kayed R, Saido TC, Bayer TA. 2007. Age-dependent axonal degeneration in an Alzheimer mouse model. Neurobiol Aging 28:1689-1699.

Woodruff RH, Franklin RJ. 1999. Demyelination and remyelination of the caudal cerebellar peduncle of adult rats following stereotaxic injections of lysolecithin, ethidium bromide, and complement/anti-galactocerebroside: a comparative study. Glia 25:216-228.

Figure legends

Figure 1. Phenotype of GPR17-expressing cells in the adult cortex. A-B': in the intact cortex, cells with either intracellular (Gpi type, arrows) or radiate (Grm type, arrowheads) GPR17 staining displayed Olig2 positivity in both gray (A,A') and white matter (B,B'). However, GPR17+/Olig2+ cells represented only a fraction of all Olig2+ cells (A,B). C,E, C-G: intracellular GPR17 spots belonged to NG2- (red in C, single confocal plane, and E, cell in vitro) and PDGFRa- (red in G, single confocal plane) expressing cells while diffuse somatic punctate staining corresponded to neurons (D). It often localized to the Golgi apparatus (red in F, immunostained with anti-GS28 antibody) or included also the starting segments of 1 or 2 cell processes (arrowhead in F'). H-I': NG2 positive Grm cells (labelled by anti-AN2 antibody) with distinct morphologies and receptor expression levels. J-K: Grm cells with intense receptor staining and broad radiating processes express premyelination markers. M,N: no colocalisation was found between GPR17 and markers for mature oligodendrocytes, such as GST-π (M) and PLP1 (N). Micrographs are confocal stacks comprising 15-20 optical sections 1mm thick. Somatic yellow pixels in J,K resulted from the overlapping of distinct optical images. L: quantifications of fractions of double positive cells over the GPR17 expressing subsets. DAPI (blue) counterstains nuclei. The dotted line in (B) indicates the boundary between gray and white matter. GM, gray matter; WM, white matter; Gpi, intracellular GPR17 protein; Grm, GPR17 receptor on cell membrane. Scale bars: 50 µm in A, B; 10 µm in B'-K; 20 µm in A', M, N.

Figure 2. Phenotype of GPR17-expressing cells during postnatal development. A-B': GPR17

is expressed in a subset of Olig2+ cells in the immature cerebral cortex. Both Grm (B) and Gpi (B') cell types were present among postnatal GPR17+ cells. C: virtually all GPR17+ cells coexpressed NG2. D: cells with intracellular GPR17 protein exhibited PDGFRa positivity. E, G: cells with high levels of receptor expression were stained also by anti PLP/DM20 (E, E') or CD9 (G, G') antibodies. H-K: no colocalisation was found with markers for mature oligodendrocytes, such as GST-π (H), PLP1 (I), MAG (J) and MBP (K). Some GPR17 processes run in parallel and intercalated with SMI32+ axons (F, F') and myelin tracts (J-K'). Micrographs are confocal stacks comprising 15-20 optical sections 1μm thick. Yellow pixels in H-J resulted from the overlapping of distinct optical images. No marker colocalisation was found in single optical sections. All micrographs are obtained from P14 cortex, with the exception of (C) obtained from a P7 brain. Arrowheads in (H) indicate neurons labelled by anti-GPR17 antibody. DAPI counterstained nuclei. Scale bars: 50 μm in A, C, F, H-K; 20 μm in B; 10 μm in D, E, G; 5 μm in B'.

Figure 3. Maturation pattern of postnatal GPR17 positive cells. A-D': changes in GPR17 and MBP expression from birth to adult stages. GPR17-positive cells were already present at birth (A). GPR17 expression increased over time (B,C) and declined in the adult cortex (D). MBP protein was instead not detectable until P7 (A',B'), whereas its expression level augmented at later time points (C',D'). E,F: graphs illustrate changes in GPR17- and GST-π-positive cell densities and anti-MBP staining intensity during postnatal development in GM (E) and WM (F). Only GPR17-/Olig2-positive cells were included in these quantifications. Densitometric quantifications of MBP labelling were normalized over P0 values: the increase in GPR17 positive cell number (P7 vs. P0, $P<0.05$) precedes GST-π/MBP rise. Its subsequent decrease (P24 vs. adult, $P<0.05$) parallels oligodendrocyte maturation. Asterisks indicate statistically

significant differences in GPR17+ cell densities compared to P0 values (One way Anova, *P*<0.05). G: quantitative analysis of the fractions of GPR17-expressing Olig2-positive/GST-π-negative cells at distinct postnatal ages. H,I: cells displaying GPR17 staining in the ramifications were very rare at birth but progressively increased amongst all receptor+ cells at postnatal ages (*P*<0.001, all postnatal ages vs. P0; Chi-square test). J: western blot analysis of GPR17 and MAG proteins revealed the presence of GPR17 before MAG production has started. Furthermore, GPR17 protein appeared downregulated before massive MAG protein production. The blot is representative of three independent experiments. P, postnatal day, GM, gray matter; WM, white matter; Gpi, GPR17 intracellular; Grm, GPR17 on cell membrane; KDa, kilodalton. Dotted lines, WM-GM border. Scale bars: 50 μm.

Figure 4. GPR17 expression in immature NG2-expressing cells during the fourth week of life. A-A': at P24, GPR17 was found in the large majority of NG2 expressing cells. Arrowheads indicate GPR17-/NG2-double positive cells. B: quantifications of fractions of double positive cells over the GPR17 expressing subsets. C,C': representative example of colocalisation between NG2 and PLP/DM20 in gray matter (confocal stack comprising only 3 optical sections 1μm thick). DAPI (blue) counterstains nuclei. Scale bars: 20 μm.

Figure 5. Proliferative activity of GPR17 expressing cells and GPR17 induction in adult newly generated NG2+ cells. A,B: proportions of BrdU+ cells amongst GPR17+ and NG2+ cells in gray and white matter. Asterisks highlight statistically significant differences between GPR17- and NG2-positive proliferative fractions (*P*<0.05). BrdU was administered for 1, 3, 7 days in the drinking water before animals were sacrificed. C-C''': cells with somatic localization of GPR17 can actively divide in the adult intact GM as shown by both anti-Ki67 (green fluorescence) and

anti-BrdU (white) staining. D,E: histograms represent the densities of cells positive for Ki67 or

for BrdU incorporated after a double pulse, and the corresponding fractions of GPR17-double

positive cells in gray (D) and white matter respectively (E). H,I: timing of GPR17 induction in

fast proliferating cells labelled by a double BrdU pulse. GPR17 was detected in about half of

the newborn cells but its expression declined over time. J,K: a similar pattern of receptor

induction was found when monitoring GPR17 expression in a larger pool of both fast and slow

proliferating cells tagged by a continuous BrdU administration for 2 weeks. F,G,L,M:

micrographs illustrate GPR17+ cells retaining BrdU after 2 or 10 weeks. Asterisks indicate

significant statistical differences in GPR17+/BrdU+ cell densities between distinct time points

(One-way Anova; *P*<0.05). Arrowheads in (F,G,L,M) indicate GPR17-/BrdU- double positive

cells. h, hours; d, days, wks, weeks. Scale bars: 10 μm in C, 50 μm in F,G,L,M .

Figure 6. GPR17 reactivity after cortical stab-wound. A-D: micrographs show anti-GPR17

labelling in the intact cortex (contralateral hemisphere, A) and in the stab-wounded tissue (B-

D) at different days post lesion (dpl). Immediately after damage, GPR17+ cells decreased in

number (B, 1dpl), but increased again at later time points (C, 7dpl). At 30 dpl the density of

GPR17 positive cells appeared similar to that of the intact condition (D). E,H: post-injury

changes of GPR17- or NG2- positive cell densities in gray (E) and white (H) matter territories.

Asterisks indicate statistically significant differences (One way Anova, *P*<0.05) in post-lesion

GPR17+ cell densities compared to intact values. F,I: cellular localization of GPR17 staining

after lesion in gray (F) and white (I) matter. Asterisks in (F) indicate a significant difference in

the percentage of cells with labelling in both somata and ramifications compared to the intact

condition (Chi-square test; ** *P*<0.01; *** *P*<0.001). G,J: BrdU incorporation in GPR17- or

NG2-positive cells after stab-wound, during 1 week of BrdU delivery in drinking water. Asterisk

in G highlights the difference (t-test, *P*<0.05) between the BrdU incorporating fractions of all GPR17+ and NG2+ cells (gray matter, 1dpl). CTRL, contralateral; SW, stab-wound; dpl, days post lesion, Gpi, GPR17 intracellular; Grm, GPR17 on cell membrane. Solid lines, lesion track; dotted lines, gray/white matter boundary. Scale bars: 50 μm.

Figure 7. GPR17 reactivity upon chronic amyloidosis. A,B: GPR17 expression in wild-type animals and age-matched APPPS1 mice. B': GPR17+ cells were found close to β-amyloid plaques (blue), where also reactive microglia (red) was detected. C: histograms depict the increase in GPR17+ and NG2+ cell densities in the gray matter (GM) of APPPS1 animals compared to wild type ones. Asterisks point to statistically significant differences (t-test, *P*<0.05). D: proportions of GPR17 positive cells with intracellular or diffuse (soma and processes) receptor localization in wild type and APPPS1 mice within 50 μm from plaques or in more distant gray matter parenchymal areas. At difference with the wild type parenchyma and with areas far from the plaque border, the vast majority of cells displayed high GPR17 in the processes (Grm) close to amyloid aggregates. Asterisks indicate the significant increase in the Grm fraction in the vicinity of plaques compared to wild type values (Chi test, *** *P*<0.001). E: BrdU incorporation in GM GPR17- or NG2-positive cells of wild type and APPPS1 mice after 1 week BrdU administration in the drinking water. While NG2 positive cells maintained a proliferative activity similar to that of wild type mice, BrdU incorporation almost doubled in GPR17 positive cells of APPPS1 animals. Asterisk highlights statistically significant difference (t-test, *P*<0.05). WT, wild type; Gpi, GPR17 intracellular; Grm, GPR17 on cell membrane. Scale bars: 50 μm.

This is the author's final version of the contribution published as:

The publisher's version is available at:
http://onlinelibrary.wiley.com/doi/10.1002/glia.21237/abstract

When citing, please refer to the published version.

Link to this full text:
http://onlinelibrary.wiley.com/doi/10.1002/glia.21237/full